Master's thesis

NTNU
Norwegian University of Science and Technology
Faculty of Natural Sciences
Department of Materials Science and Engineering

Morten Steinsmo Dybdahl

Hybrid Nanocomposites for High Voltage Insulation

Master's thesis in Chemical Engineering and Biotechnology
Supervisor: Mari-Ann Einarsrud,
Co-supervisor: Mohammed Mostafa Adnan
July 2019

NTNU
Norwegian University of
Science and Technology

Morten Steinsmo Dybdahl

Hybrid Nanocomposites for High Voltage Insulation

Master's thesis in Chemical Engineering and Biotechnology
Supervisor: Mari-Ann Einarsrud,
Co-supervisor: Mohammed Mostafa Adnan
July 2019

Norwegian University of Science and Technology
Faculty of Natural Sciences
Department of Materials Science and Engineering

NTNU
Norwegian University of
Science and Technology

Preface

This thesis markes the end of my time as a part of the masters program Chemical Engineering and Biotechnology at NTNU, Trondheim. The work was carried out at the Department of Materials Science and Engineering during spring of 2019. This last semester has been filled with both prosperity and adversity, and I'm left with an eternal gratitude for all the help and guidance I have received.

First I would like to thank my supervisor Professor Mari-Ann Einarsrud for guidance and help, and for creating an pleasant environment during our weekly meetings. I would also like to express my greatest gratitude to my co-supervisor Mohammed Mostafa Adnan for invaluable help, support and assistance during this period, and for always taking the time to help me.

I will also give a special thanks to the staff at Department of Materials Science and Engineering at Kjemiblokk II for help related to training, and for helping me when 'needed.

Trondheim, July 15, 2019

Morten Steinsmo Dybdahl

Abstract

The use of nanoparticles as filler material in organic polymers has proven to enhance desired properties in the polymer for high voltage insulation. There exist many different methods for the preparation of hybrid nanocomposites today, but they all face the same challenge; how to get a homogeneously dispersion of the filler material. In this thesis epoxy-TiO_2 nanocomposites were prepared *in situ* with the use of the sol-gel method. Samples with 1, 2, 3, 4 and 5 wt % of filler content were prepared, through hydrolysis and condensation of the metal precursor titanium(IV)isopropoxide. The purpose of preparing the samples *in situ* is to grow them directly inside the polymer, avoiding the challenges by mixing already prepared nanoparticles with the polymer. The prepared samples were characterized to see if there were any changes in the properties of the composite material compared to the neat epoxy.

The formation of TiO_2 particles was confirmed by Fourier-transform infrared spectroscopy, and also thermogravimetric analysis, as one can assume that the remaining mass after the pyrolysis, which exeeded the temperature of decomposition for polymers, were inorganic material (TiO_2 particles). Raman did show peaks indicating the presence of TiO_2, but the same peaks appeared for the neat epoxy. This might be due to to small amounts of TiO_2 to be detected. The glass transition temperature were found to be close to the one for neat epoxy, around 90 °C, with most samples showing a higher glass transition temperature.

The relative permittivity was found to decrease with higher frequency, and the relative permittivity of the prepared composites did not differ significantly from the relative permittivity of the neat epoxy. The dielectric loss tangent increased at lower frequency for the composites compared to the neat epoxy, but at higher frequency the trend shifted, and the neat epoxy showed the highest dielectric loss. The SAXS measurements showed that there was indeed agglomerates, preferably of TiO_2, in the composite, but there was not sufficient data to confirm that it was TiO_2 particles.

Sammendrag

Bruken av nanopartikler som fyllmateriale i organiske polymerer har vist seg å forbedre ønskede egenskaper i polymerer for høyspenningsinsolasjon. Det eksisterer mange ulike metoder for forberedelse av hybride nanokompositter i dag, men de står alle ovenfor samme utfordring; hvordan få en homogen dispersjon av fyllmaterialet. I denne avhandlingen ble epoksy-TiO_2 nanokompositter forberedt *in situ* ved bruk av sol-gel metoden. Prøver med 1, 2, 3, 4 og 5 vektprosent fyllmaterial ble forberedt gjennom hydrolyse og konsendasjon av metallforløperen titan(IV)isopropoksid. Formålet med å forberede prøvene *in situ* er å dyrke TiO_2-partiklene direkte inn i polymerer, og med det unngå utfordringen ved miksing av allerede forberedte nanopartikler med polymeren. De forberede prøvene ble så karakterisert for å se om det var noen endringer i egenskapene hos kompositttmaterialet sammenlignet med ren epoksy.

Dannelse av TiO_2-partikler ble bekreftet Fourier-transform infrarød spektroskopi, og også ved termogravimetrisk spektroskopi, da det kan antas at gjenværende masse etter pyrolyse, hvilket overgikk dekomponeringstemperaturen for polymerern, var uorganisk material (TiO_2-partikler). Raman spektroskopi viste topper som indikerer tilstedeværelse av TiO_2, men de samme toppene viste seg for ren epoksy. Dette kan være grunnet for små mengder av TiO_2, slik at det ikke detekteres. Glasstemperaturen ble funnet å være nær temperaturen for ren epoksy, der de fleste prøvene viste en høyere glasstemperatur.

Den relative permittiviteten ble funnet å avta med høyere frekvens, og den relative permittiviteten hos de forberedte prøvene avviket ikke betydelig fra den relative permittiviteten hos ren epoksy. Tangenten for dielectrisk tap økte ved lavere frekvenser for komposittene sammenlignet med ren epoksy, men ved høyere frekvenser shiftet denne trenden, og ren epoksy hadde høyest tangent for dielektrisk tap. SAXS-målingene viste at det riktignok var agglomerater, fortrinnsvis TiO_2, i komposittene, men det var ikke tilstrekkelig med data for å bekrefte at det vart TiO_2-partikler.

Contents

1 Background

1.1 Motivation

In the resent years increased interest in the use of inorganic materials at nanoscale to improve selected properties of organic polymer materials has been observed. Increased interest due to the different behaviour materials exhibit at nanoscale, compared to at microscale and in bulk [1]. These hybrid materials, a combination of an inorganic and an organic material, are called nanocomposites. Nanocomposites used as electrical insulation materials in high voltage equipment benefit from the properties from both the inorganic and the organic material, without altering the composition of the materials. Whilst organic polymers, such as epoxy, possesses outstanding electrical insulating, thermal and mechanical properties, they are also very cheap materials which are easy to shape into the desired forms. The problem with polymers is that they are brittle, and the incorporation of inorganic particles (microscale and bulk) has shown to increase selected mechanical properties, but at the cost of some of the electrical properties, such as permittivity and breakdown strength. The use of the inorganic materials at nanoscale has shown to be promising, as improved mechanical properties has been observed, while at the same time the desired electrical propetries of the polymer remains unaltered. This is due to the large to surface area of nanoparticles compared to particles of larger sizes (microscale and bulk).

The processing of nanocomposites has been done through both *ex situ* and *in situ* synthesis methods. *Ex situ* methods involves the incorporation of pre-synthesized particles inside the host material. *In situ* synthesis allows preparation of a material using a precursor which generates the growth of particles directly inside the host material. The main challenge during the synthesis of nanocomposites is to obtain a homogeneously dispersion of the nanoparticles in the polymer.

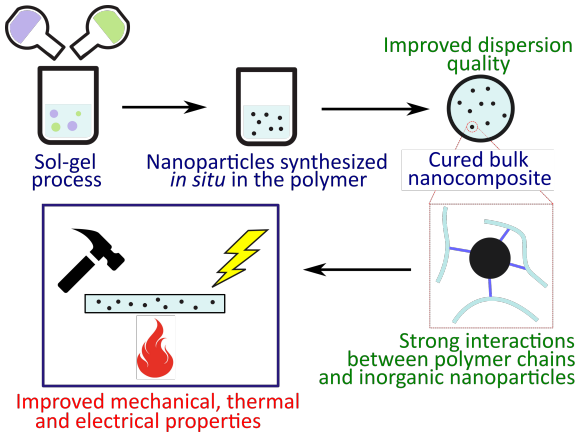

Figure 1: The purpose of this work is to apply the sol-gel method to obtain hybrid nanocomposites, which will be characterized based on properties of interest [2].

1.2 Aim

Further, the aim of this work is to develop an *in situ* synthesis route base on sol-gel chemistry to prepare TiO_2-epoxy nanocomposites. Further, the aim is to increase both the glass transition temperature and the degradation temperatureof the epoxy, and at the same time preserve good dielectric properties. The obtained nanocomposites will be synthesized with varying amounts of TiO_2 nanoparticles; 1, 2, 3, 4 and 5 wt%, and the effect of the different amount of filler content will be investigated.

The prepared samples will be characterized based on their phase composition, glass transition temperature, degradation temperature, relative permittivity, and dielectric losses.

2 Introduction

2.1 Nanomaterials

The great interest for nanomaterials that has emerged during the last decades is due to the different properties compared to bulk materials, but also materials at micro scale. Nanomaterials are defined as materials where 50 % or more of the particles in the material is in the range of 1-100 nm [3]. For bulk materials, the number of surface atoms becomes negligible compared to the total amount of atoms, and they will therefore have little influence on the properties of the material. For nanomaterials however, where the size is significantly smaller as shown in Figure 2, the proportion of surface atoms compared to total amount of atoms becomes significant, which gives rise to different properties compared to the bulk materials [4].

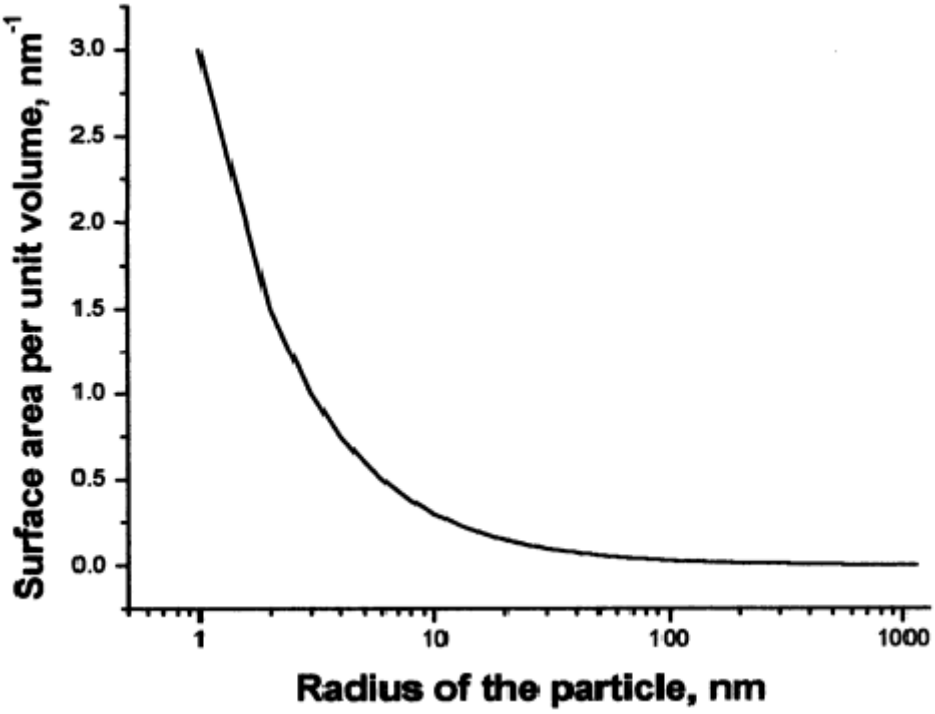

Figure 2: Illustration of surface area per unit volume as a function of the particle size [5].

The large surface area of nanoparticles gives rise to large surface energies, promoting agglomerations.

2.1.1 Synthesis of nanomaterials

When synthesizing nanomaterials there are two different approaches that can be used, bottom-up and top-down, as shown in Figure 3.. For chemical bottom-up approach, the nanomaterial is synthesized from atoms and molecules at the nanoscale. The atoms and molecules are arranged together through e.g. self-assembly, to build the desired nanomaterial. Physical bottom-up methods includes different deposition techniques, such as atomic layer deposition (ALD), molecular beam epitaxy (MBE) and physical vapor depostion (PVD). The desired material is in this case deposited at a substrate with controlled properties. Chemical bottom-up methods include the preparation of nanomaterials using chemical solutions or colloids. Sol-gel, hydrothermal synthesis and electrodeposition (ED), are some of these methods [6]. In top-down approach, bulk materials at microscopic or macroscopic size, are whittled down to nanometric dimensions. Several litography techniques, such as nanolithography (NL) and electron beam lithography (EBL), but also other techniques such as inject printing and arc discharcge (AD) [7].

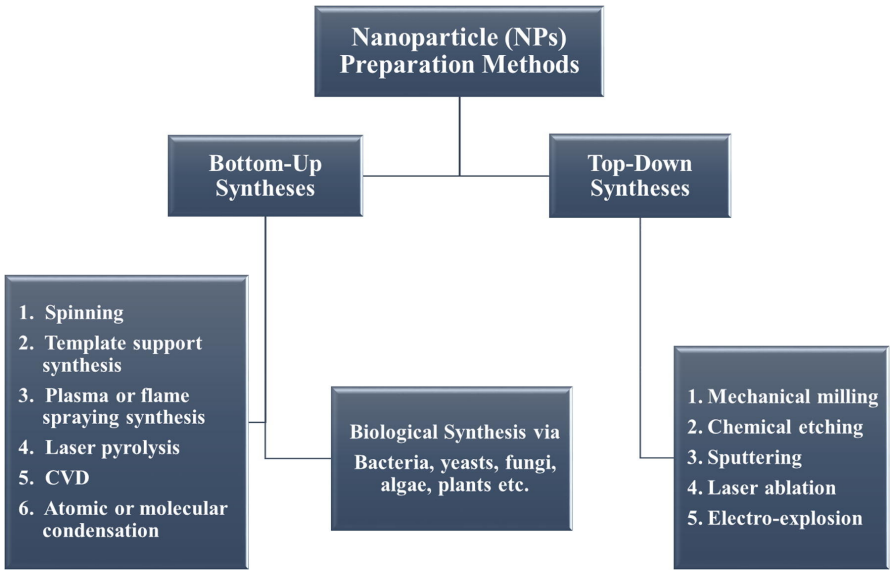

Figure 3: The two main approaches for preparation of nanoparticles, (1) bottom-up and (2) top-down [7].

2.1.2 Nanofiller for nanocomposites

2.1.2.1 TiO_2

Titania (TiO_2) is a semiconducting material with a wide band gap, and thus an interesting material for energy applications. TiO_2 is chemically stable, versatile when it comes to functionality, and environmentally compatible oxide [8].

After Fujishima and Honda observed the possibility of photocatalytic splitting of water on a TiO_2 electrode, there has been done a lot of research on the appications of TiO_2 for both environmental and energy technologies [9]. The properties of TiO_2 depend on several factors, such as size of particles, crystal structure and modifications of the surface. These properties are not the only thing the applications depend on, as the interactions between TiO_2 and other materials, such as polymers, and the modifications of TiO_2 also plays a big role [10]. TiO_2 is widely used as pigment, in sunscreen and paint, and also as food coloring.

There is a total of eleven different polymorphs of TiO_2 that have been observed,

in either bulk or nanocrystalline phase, or both. They are listed in Table 1. The most common polymorphs is shown in Figure 4, and are anatase, rutile and brookite, and they are known to occur naturally, while the other ones are usually synthesized [8]. Rutile is the most stable of the three common structures at larger size [11], but below 30 nm the anatase phase becomes mor stable than rutile. This is due to the lower surface energy of anatase compared to rutile. The stability is an effect of the increasing importance of surface energies at smaller particle sizes. Brookite is quite rare to find naturally, and also difficult to synthesize. Rutile and anatase are therefore the most preferred phases of TiO_2 for industrial applications [12].

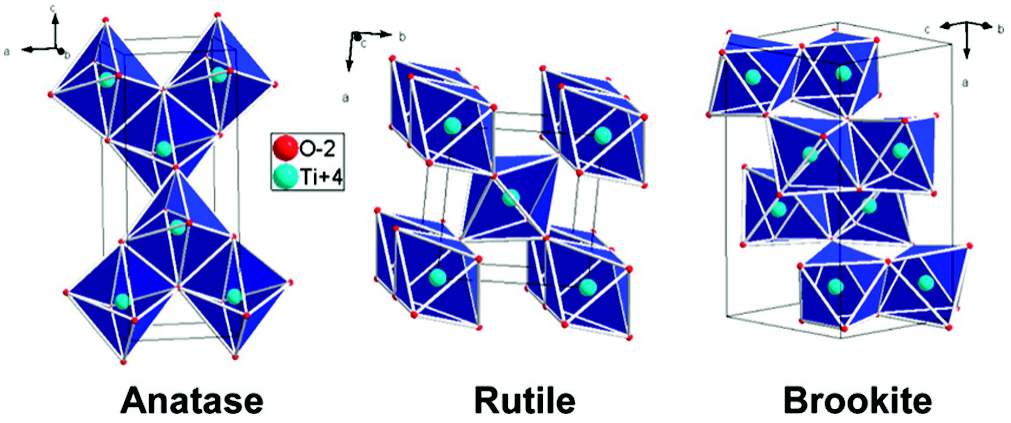

Figure 4: Structures of the most common polymorphs of TiO_2; Anatase, rutile and brookite [13].

Table 1: The different phases, and their crystal structures of TiO_2 [8].

Phase	**Crystal system**	**Note**
Rutile	Tetragonal	Stable at ambient or low pressure
Anatase	Tetragonal	
Brookite	Orthorhombic	
TiO_2(B)	Monoclinic	
TiO_2(H)	Tetragonal	
TiO_2(R)	Orthorhombic	
TiO_2(II)	Orthorhombic	High pressure phase
Baddeleyite	Monoclinic	
OI	Orthorhombic	
OII	Orthorhombic	
Cubic	Cubic	

2.2 Polymer materials

Polymers are chainlike structures which consist of a large number of simple molecules, monomers, which can undergo polymerization [14]. Polymer materials are usually divided into three basic families; thermoplasts, elastomers, and thermosets [15]. The first family, thermoplasts, are materials that are solid at room temperature, but softens as the temperature are increased. The second family, elastomers, are flexible materials, which lies in between the glass transition temperature and the melting temperature. The last family, thermosets, are initially liquids, that upon heating forms into a solid material. They can not be re-formed upon heating, as opposed to thermoplast, and they will therefore keep their shape until degradation occurs. The reason why they do not have the ability to be re-formed is the cross-linking, which also contributes to the stability of the polymer material.

Polymers are usually classified according to the structural shape of the material, and the three different shapes are linear, branched and network, as illustrated in Figure 5 [16].

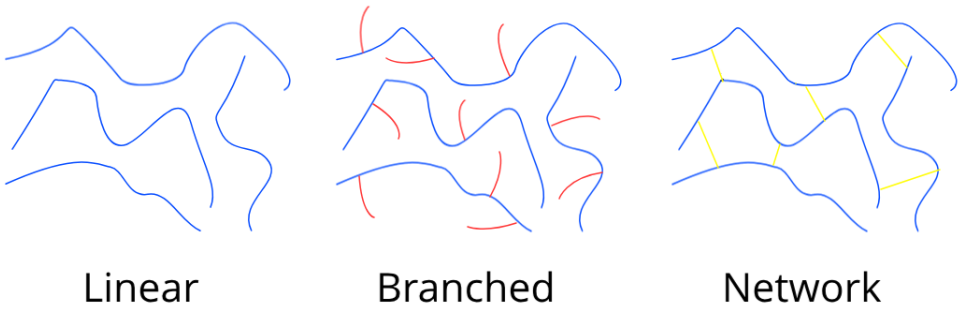

Figure 5: Illustration of the different structures polymers are classified into.

2.2.1 Epoxy resin

Epoxy resin is a thermoset, which as mentioned in the previous section, that that they cannot be re-formed upon heating. Properties such as outstanding chemical resistance, excellent electrical insulation capabilities when it comes to electrical usage, and a variation of suitable toughness properties versatile for several applications, including electrical insulation. However, poor brittleness and low thermal stability is a barrier when it comes to high voltage applications. This is also the reason why there is interest in combining the epoxy resin with an inorganic material [17]. Diglycidyl ether of bisphenol A (DGEBA), structure shown in Figure 6, is a type of epoxy resin, and the type used in the synthesis of the nanocomposite. Some of the properties of DGEBA is listet in Table 2.

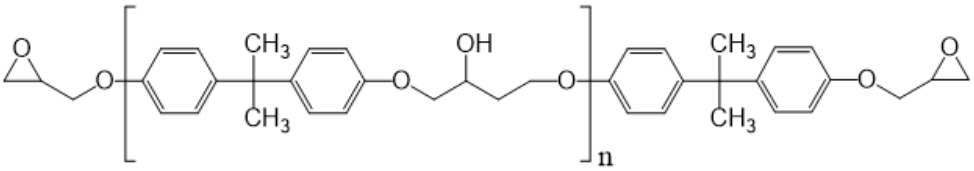

Figure 6: Chemical structure of DGEBA [18].

Table 2: Selected properties of DGEBA.

Properties	Approximate values	Reference
Relative permittivity (1 kHz)	3.52-3.55	[19]
Glass transition temperature (°C)	70-99	[20]
Dielectric breakdown strength (V/μm)	288	[21]
Thermal conductivity (W/mk)	0.1 - 0.5	[22]

Epoxy resins does not form the cross-linked network by themselves, and it is therefore necessary to use curing agents. The main purpose of the curing agent (also called hardener or crosslinker) is to promote curing of the polymer [23]. Poly(propylene glycol) bis(2-aminopropyl ether) (JeffamineD230), shown in Figure 7 is a common curing agent used for the curing of epoxy resins.

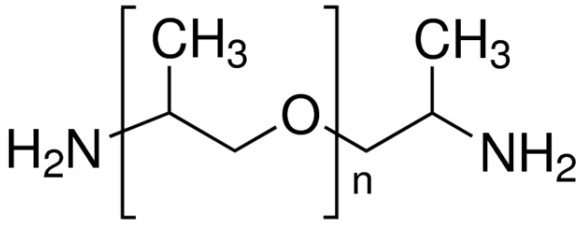

Figure 7: Chemical structure of the curing agent Poly(propylene glycol) bis(2-aminopropyl ether) [24].

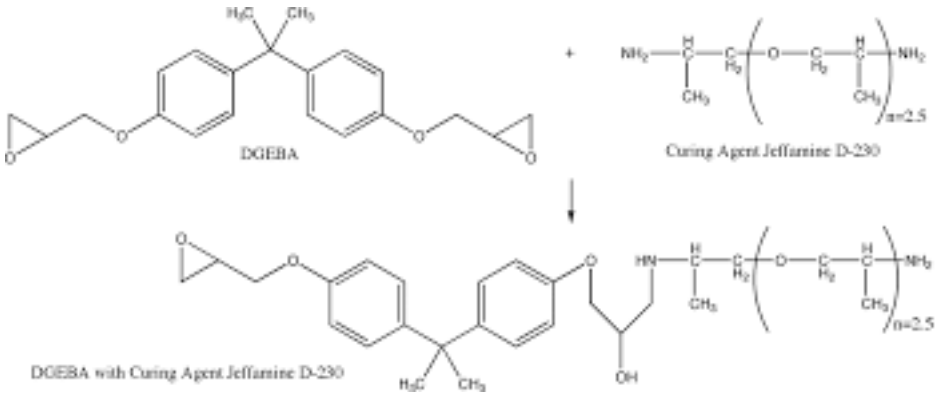

Figure 8: Curing reaction between the polymer, diglycidyl ether of bisphenol A, and the curing agent, Poly(propylene glycol) bis(2-aminopropyl ether [25].

2.3 Nanocomposites

Different kinds of composite materials have been of interest and studied for a long time, and due to the novel properties of nanoparticles, nanocomposites have obtained greater interest in the recent years [26]. Nanocomposites are materials which consists of two phases, where one of the phases is dispersed into the other. These are called hybrid materials, as one of the phases is an inorganic material, such as nanoparticles or other type of filler material, whilst the other phase is an organic material, such as a polymer, which work as a matrix which induces a three-dimensional network. The inorganic material is dispersed into the organic material [27]. The purpose of a composite material is to combine the different properties the inorganic (e.g. thermal stability) and the organic (e.g. ductility, dielectric) materials exhibit [26]. The properties of a nanocomposite will not only be the sum of the different contributions, but the interface between these materials will also affect the properties, and thus create new and unique properties [28]. The small size of the filler material (nanoscale) gives rise to a large interfacial area, as compared to fillers of microscale size. Nanocomposites can be derived into two different classes, depending on the nature of the interface between the different components; Class I and class II. In class I hybrids there are only weak interface bonding between the different components, such as van der Waals and electrostatic forces, and hydrogen bonding. These weak interface forces gives the only cohesion to the structure of the material. In class II hybrids, stronger forces holds the different components together, such as strong covalent bonds or iono-covalent bonds [29, 30, 31]. The two classes are illustrated in Figure 9.

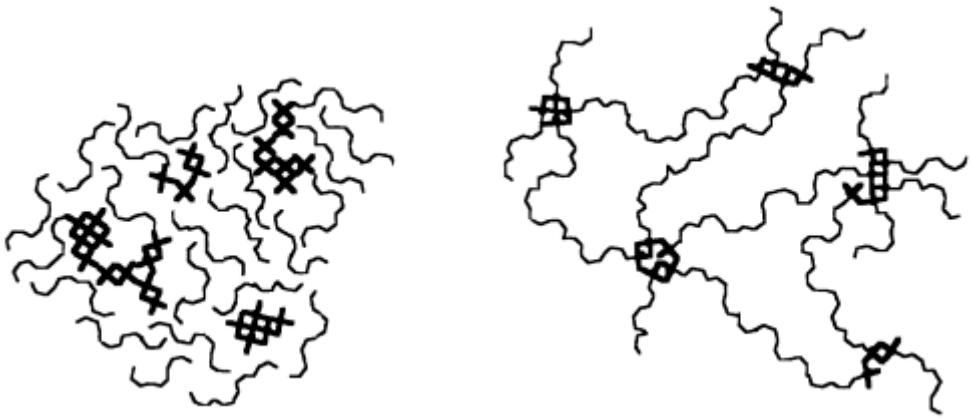

Figure 9: Illustration of class I (left) and class II (right) hybride materials. The thin threads illustrates organic chains, while the thicker threads illustrates inorganic domains [30].

As of today *ex situ* approaches are more common to use when preparing nanocomposites, as they are easy to scale up for industrial purposes. Some of the *ex situ* approaches that have been developed includes mechanical stirring to disperse the already synthesized particles [32], high shear mechanical stirring followed by ultrasonication to break apart possible formed agglomerates [33], and high impeller stirring followed by ultrasonication [34].

Nanocomposites prepared by in situ are not as common as *ex situ* synthesized nanocomposites, as it is more complicate for upscaling. Techniques such as reverse microemulsions , solvothermal synthesis, and sol-gel chemistry involving the use of a precursor have been used to prepare nanocomposites *in situ* [35, 36, 28]. It usually involves the reaction of the precursor which then initiates the growth of the particles.

2.3.1 *Ex situ* synthesis of nanocomposites

When using the *ex situ* synthesis to produce polymer nanocomposites, the inorganic nanoparticles are synthesized first. After the inorganic material is synthesized separately and isolated from the organic material, the two materials are then mixed together, either by blending the inorganic particles in the polymer, or by adding them

to the monomer by *in situ* polymerization, as presented in Figure 10. By preparing the particles before adding them to the solution there is easier to control the properties of them, such as size distribution and functionalisation. One of the main challenges with the *ex situ* synthesis is the difficulty of controlling the degree of dispersion, which one desires to be homogeneous. The degree of dispersion may be enhanced by surface modification of the particles [37].

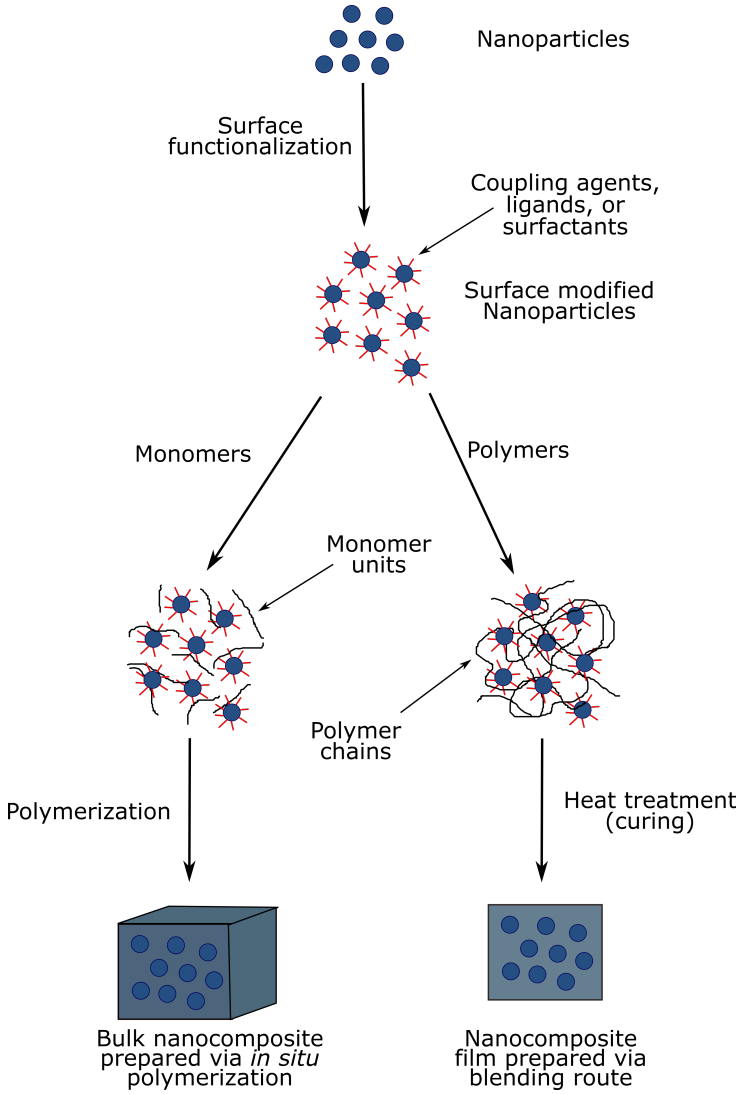

Figure 10: Illustration of *ex situ* synthesis of nanocomposites [24].

2.3.2 *In situ* synthesis of nanocomposites

When using the *in situ* synthesis to produce polymer nanocomposites, the inorganic material is synthesized directly inside the polymer. The main advantage using this method rather than using the *ex situ* approach is that the dispersion becomes more homogeneous.

The sol-gel method is used to produce hybrid materials, such as inorganic polymer materials or ceramics. First a solution containing a desired precursor and a solvent goes through chemical reactions, usually hydrolysis and condensation, to form a *sol*, before transforming the *sol* to a *gel*. The *gel* is a network structure, bridged by the connections between the inorganic and organic materials. After the formation of the *gel*, the solvent is removed. Ceramic fibers, dense films and powders are some of many materials that can be achieved by using the sol-gel method, as illustrated in Figure 11 [38].

As mentioned, sol-gel method is used to produce hybrid materials, and is therefore one of the most common synthesis routes used when performing a *in situ* synthesis of hybrid nanocomposites. This is mostly due to the fact that (1) there is no need for high temperatures when using the sol-gel method, and (2) the introduction of a precursor directly into the monomer of the polymer at a early stage, contribute a homogeneously dispersion of the nanoparticles [39].

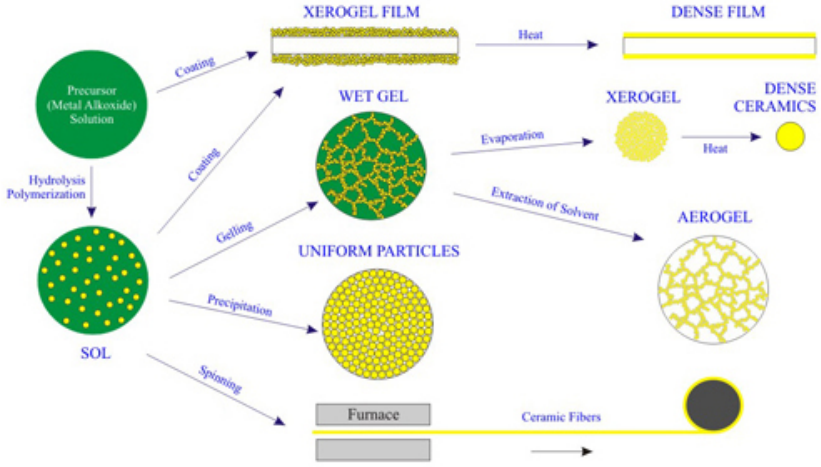

Figure 11: Flow chart of the versatility of the sol-gel synthesis [40].

The *in situ* sol-gel synthesis, is a synthesis consisting of two steps. (1) the metal precursor goes through hydrolysis (Figure 12) with the purpose of attaching hydroxyl groups to the titanium atom.

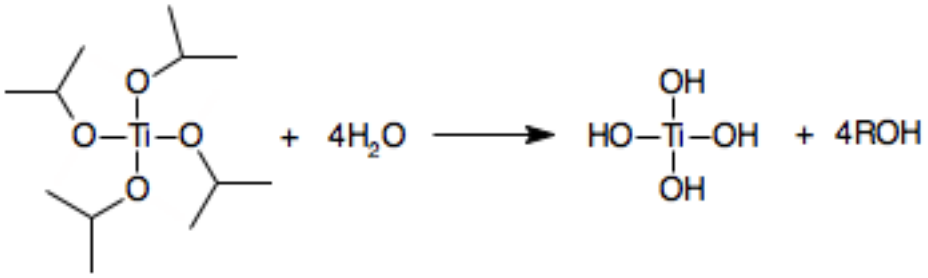

Figure 12: The hydrolysis of the titanium precursor; titanium(IV)isopropoxide.

(2) the hydroxyl groups attached to the titanium atom, and the alkoxy groups goes through polycondensation (Figure 13 to form the inorganic polymer network.

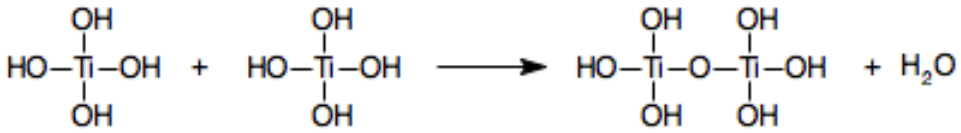

Figure 13: The polycondensation of the titanium(IV)isopropoxide precursor, where the alkoxy groups are replaced by hydroxyl groups.

When metal alkoxides are used as precursor, the total reaction, where the precursor react through step (1) and (2) to give a metal oxide is given as;

$$\mathrm{M(OR}_z + \frac{1}{2}\mathrm{H_2O} \xrightarrow[\text{Polycondensation}]{\text{Hydrolysis}} \mathrm{MO_{z/2}} + \mathrm{zROH} \tag{1}$$

where M is a metal with oxidation number z, OR an alkoxy group where oxygen is attached to a alkyl group, R. The entire *in situ* sol-gel synthesis of epoxy-TiO_2 nanocomposite is shown in Figure 14

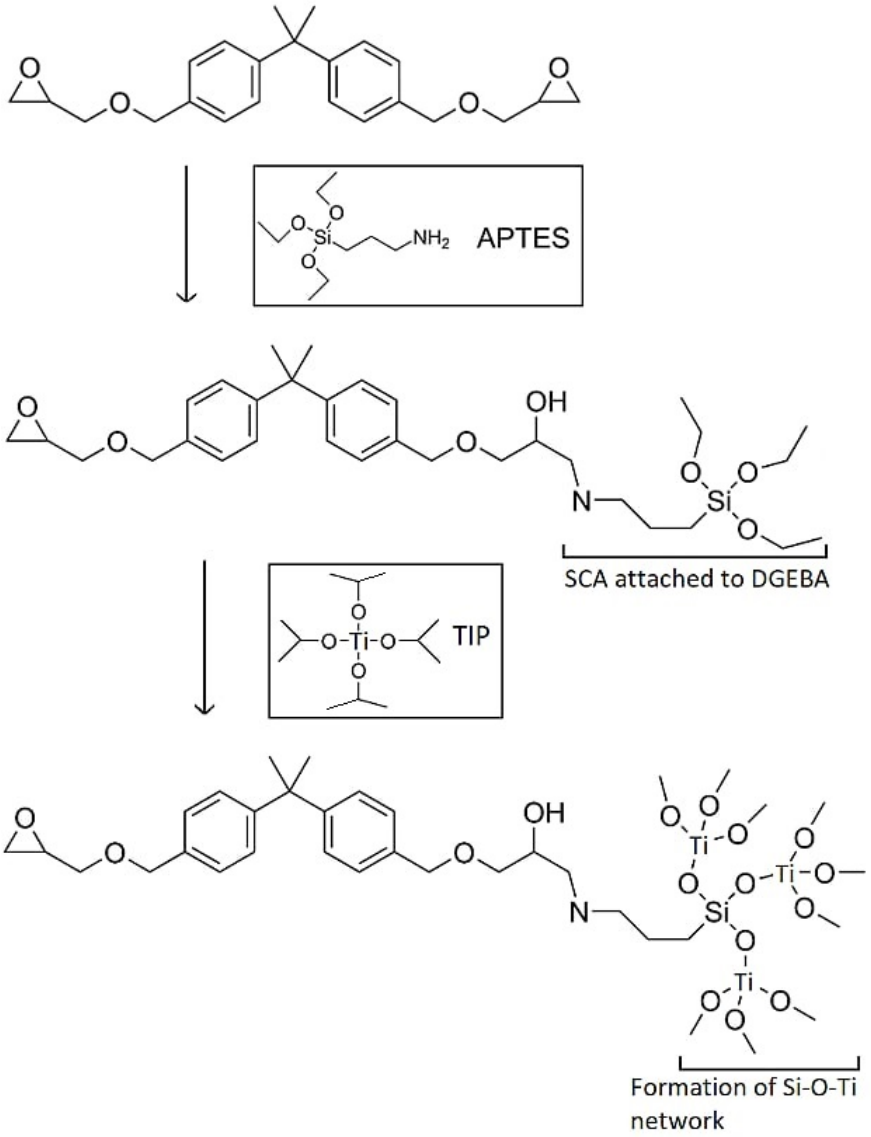

Figure 14: Schematic of the sol-gel synthesis of epoxy-TiO_2 when using (3-Aminopropyl)triethoxysilane (APTES) as a coupling agent, and titanium(IV)isopropoxide (TIP) as precursor.

2.4 Silane coupling agent

The dispersion of the nanoparticles in the polymer matrix is one of the main challenges when synthesizing nanocomposites, as the nanoparticles tends to agglomerate. Surface modifications are often carried out to improve the quality of dispersion [18]. Surface modifications can be done in two ways, (1) physically or (2) chemically. Physical modifications are based on addition of polymers onto the surface of the nanoparticles. The two materials are coupled as a result of covalent bonding. Chemical modifications are accomplished through formation of chemical bonds by either surface adsorption on the nanoparticles, or by coupling of the nanoparticles with an molecule, which can be a coupling agent [41]. The first approach gives more control over the properties of the nanoparticles, while the second approach is more stable, as the first one involves formation of weak van der Waals forces.

Silane coupling agents are molecules that can be used to modify the interface between the inorganic and the organic materials, and thus improve the coupling of the different materials. The most common silane coupling agents have three hydrolyzable groups attached to the silicon atom (X). These groups are usually either alkoxy, amine or halogen. One organic group (R), is also attached to the silicone atom. The structure of a general siliane coupling agent is shown in Figure 15 [42].

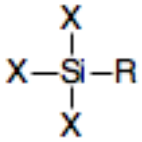

Figure 15: Schematic of the standard chemical structure of an silane coupling agent. X indicates the hydrolyzable groups, while R indicates organic groups.

The advantages of silane coupling agents are [43];

- Available in large scale
- Have alkoxy groups that can react with OH

- Have functional groups that can be tailored to be compatible with different type of matrixes

There are many different types of silane coupling agent, and therefore it is important to choose a type that suits the materials characteristics. Some features that should be considered when selecting a silane coupling agent is;

- Which type of bonds, and the stability of the bands between the inorganic and the organic phase
- What group of the organic material that works as the functional group
- Which type of hydroxyl group the precursor consist of
- Amount of hydroxyl groups attached to the precursor

In Figure 16 the structure of (3-Aminopropyl)trimethoxysilane (APTES) and (3-Glycidyloxopropyl)trimethoxysilane (GPTMS) is shown. These two silane coupling agents are suited when using a epoxy resin such as DGEBA.

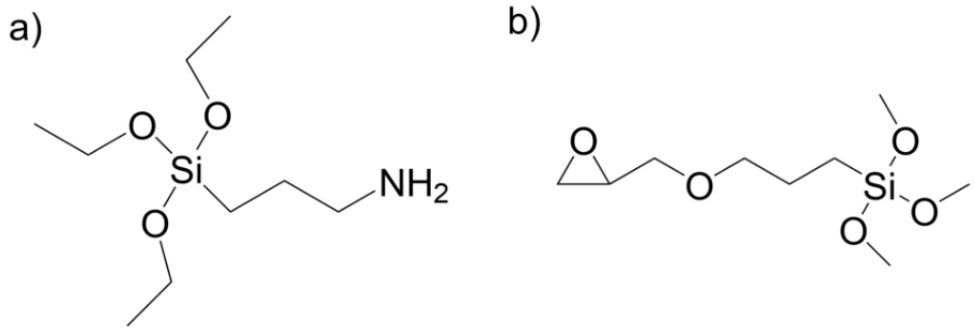

Figure 16: Chemical structures of a) APTES and b) GPTMS [24].

2.5 Thermal properties

Temperature, and therefore the thermal properties of nanocomposites with polymers, are crucial for their behaviour. This is especially important for high voltage insulation, where heat transfer, caused by dielectric losses, leads to an increase in temperature of the material.

2.5.1 Glass transition temperature

The glass transition temperature, as illustrated in Figure 17, is the temperature in which the polymer goes through a structural change, from an hard and glassy amorphous solid to a rubbery like substance.

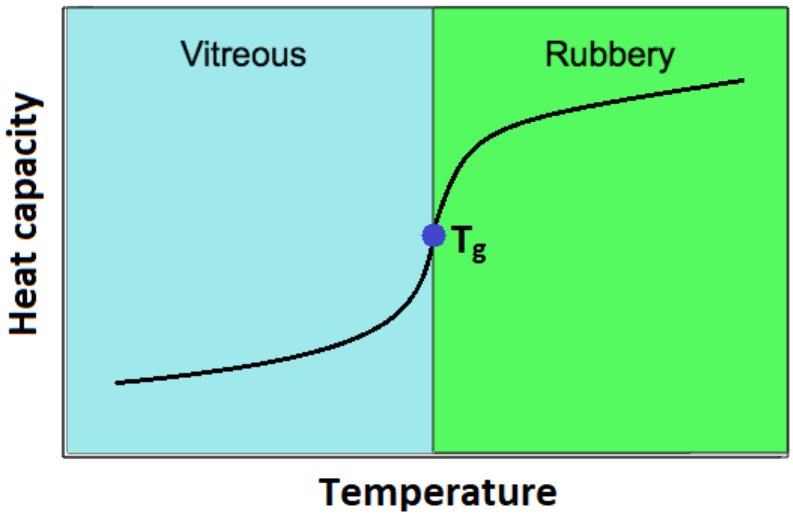

Figure 17: Illustration of the change in heat capacity illustrating the glass transition temperature..

The glass transition temperature is defined as the temperature in which a transformation occurs, while heating or cooling at a constant temperature rate. As there is no desire to have a rubbery material for a high voltage insulating material, high glass transition temperatures are desired. Table 3 shows selected values for the glass transition temperature of epoxy-TiO_2 nanocomposites.

Table 3: Glass transition temperature for different epoxy-TiO_2 composites.

Sample code	**TiO_2 (wt%)**	**Tg °C**	**Reference**
	0-10	62-80	[44]
Epoxy-TiO_2	16	85-100	[21]
	0-10	61-69	[33]

2.5.2 Degredation of nanocomposites

2.6 Electrical properties

The electrical properties of the material are of the utmost importance in terms of high voltage usage. Properties such as permittivity and breakdown strength are electrical properties that determines the insulation properties.

2.6.1 Relative permittivity

The relative permittivity (dielectric constant), give and ϵ, is an important parameter when describing dielectric materials. Relative permittivity is a measure of how a material behaves when an external field is applied. Increased relative permittivity implies higher resistance againt applied electric field. When an electric field is applied (e.g. a dielectric placed between two charged metal plates) the nuclei and electrons will move in opposite direction of eachother. The positively charged nuclei will move towards the applied electric field, while the negatively charged electrons will movie in the other direction [45]. The behaviour of the charged species depends on;

- nuclei mass
- how strong electrons are bound
- the applied electric field

In other words, the dielectric constant gives information of the strength of the material.

3 Experimental

3.1 Chemicals

Chemicals used for the synthesis are listed in Table 4.

Table 4: List of chemicals used in the synthesis of epoxy-TiO_2 - nanocomposite.

Chemical	**Function**	**Abbreviation**	**Formula**	**Purity (%)**	**Manufacturer**
Diglicydyl ether bisphenol A	Polymer matrix	DGEBA	$C_{21}H_{24}O_4$	-	Sigma- Aldrich
3-(Aminopropyl) triethoxysilane	Coupling agent	APTES	$C_9H_{23}NO_3Si$	99	Sigma-Aldrich
Titanium(IV) isopropoxide	Precursor	TIP	$C_{12}H_{28}O_4Ti$	97	Sigma-Aldrich
Poly(propylene glycol) bis(2-aminopropyl ether)	Curing agent	JeffamineD230	$CH_3CH(NH_2)CH_2$ $[OCH_2CH(CH_3)]_nNH_2$	-	Sigma-Aldrich
Isopropanol	Solvent	-	C3H8O	99.5	Sigma-Aldrich

3.2 Synthesis method

The experimental setup for the synthesis of the nanocomposite is shown in Figure 19

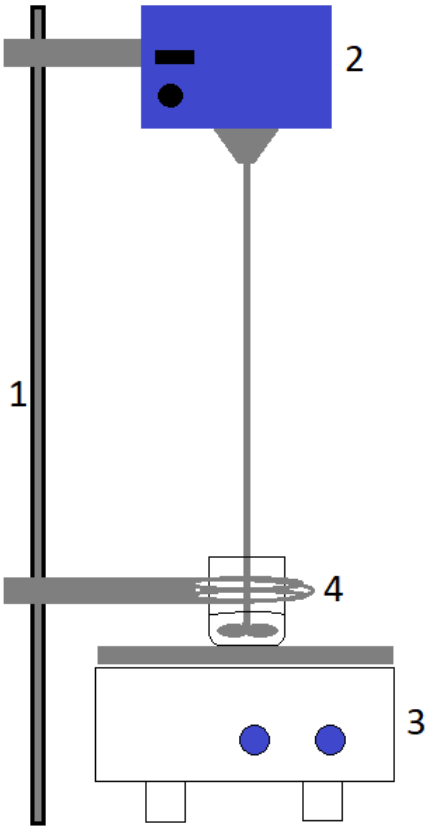

Figure 18: Set-up used for the synthesis of nanocomposites. (1) The supporting rod, (2) the mechanical stirrer attached to the rod, (3) hot plate, and (4) the beaker on top of the plate.

The final synthesis procedure, after optimizing the inititial conditions, proceeded as follow (REFERERE TIL PROSJEKTOPPGAVE). Diglycidyl ether of bisphenol A (DGEBA) (15 g) was poured into a glass beaker, and then placed on a heating plate. A mechanical stirrer was used to mix the content of the beaker at 350 rpm. The desired amount of (aminopropy)triethoxysilane (APTES) (3.56 mL) was added dropwise to the beaker. After the addition of the APTES the mixture was stirred for 1 hour. Isopropanol (6 mL) was added to a second beaker, and then placed on a magnetic stirrer. Different amounts of titanium (IV) isopropoxide (TIP), as shown in Table 5, was added dropwise to the isopropanol and stirred at 350 rpm for 5 minutes. The extraction and addition of the TIP into the isopropanol was performed under an

inert atmosphere with the use of nitrogen gas. After mixing the DGEBA and APTES for 1 hour the content of the second beaker was added dropwise, and then stirred for 4 hours, before it was heated to 90 °C, and stirred for another 3 hours.

After stirring the mixture for 7 hours poly(propylene glycol) bis(2-aminopropyl ether) (JeffamineD230) was added dropwise to the mixture, and stirred for another 15 minutes. The beaker was then put into a vacuum furnace (Binder vacuum drying furnace, VD23) for 30 minutes, and after this the content was poured into teflon molds. The molds were shaped as circles, with i diameter of approximately 30 mm. The molds were then put into the vacuum binder furnace for 1 hour, before they were put into a furnace and heated for 5 hours at 100 °C.

Table 5: Amount of titania(IV)isopropoxide used in the synthesis of epoxy-TiO_2 - nanocomposite.

wt% TiO_2	**Amount of TIP [mL]**
1	0.74
2	1.48
3	2.23
4	2.98
5	3.72

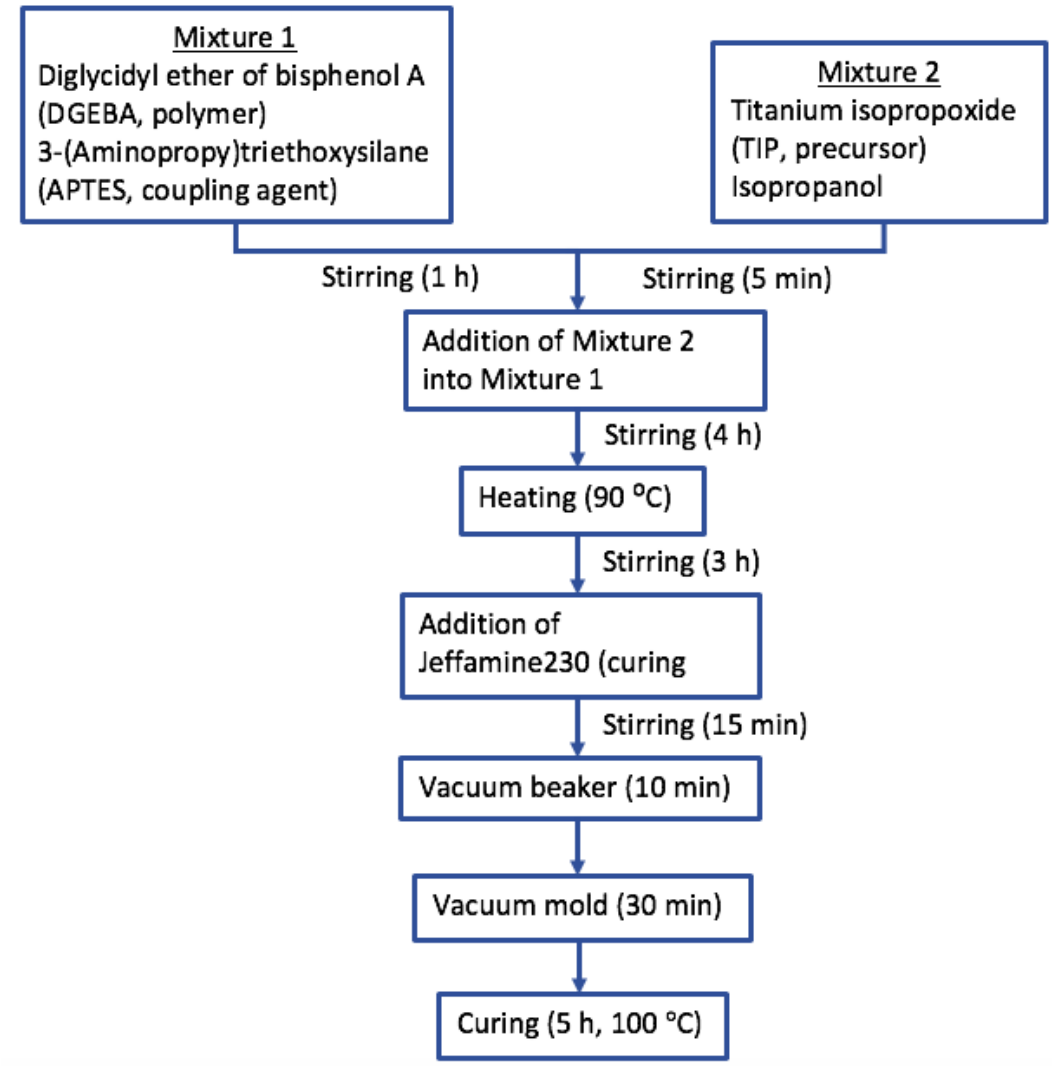

Figure 19: Flowsheet of the synthesis route used for the last samples prepared.

Table 6

Series	TIP (mL)	Stirring (h)
1wt	0.74	8
2wt	1.48	8
3wt	2.23	8
4wt	2.98	8
5wt	3.72	8
NeatEpoxy	0	2

Table 7: The samples used for the characterization, and their amount of precursor (TIP) and reaciton time.

3.3 Characterization

3.3.1 Fourier-transform infrared spectroscopy

Fourier-transform infrared spectroscopy (FTIR) was carried out using a Bruker Vertex 80v, obtaining a spectra in the range from 400 to 4000 cm^{-1}, against a vacuum background. 32 scans was acquired for each spectra, with a resolution of 1 cm^{-1}.

3.3.2 Raman spectroscopy

Raman measurements was carried out using WITec alpha 300 R. 10x and 50x were used for focusing, and the measurements were obtained at 100x magnification, and a laser with a wavelength of 532 nm. Ten accumilations of 30 seconds each were used to obtain the spectra.

3.3.3 Differential scanning calorimetry

Differential scanning calorimetry was carried out using DSC 214 Polyma Auto to obtain the glass transition temperature of the samples. A background was first collected, for an empty crucible. Before measurements of the samples, a sapphire standard was collected. The samples was weighted, put into the crucible, and then

introduced into the furnace. The samples then underwent 4 full cycles of heating and cooling. The temperatures was in the range of 0 to 200 °C, with a rate of heating/cooling of 10 °C/min. The temperature profile is illustrated on Figure 20. A sapphire standard was used against the measurements to obtain the heat capacity. 4 cycles was used, as the first one works as a burn off of eventual impurities, and the three remaining as a control to see if there is any difference between the cycles. A nitrogen atmosphere was used during the analysis.

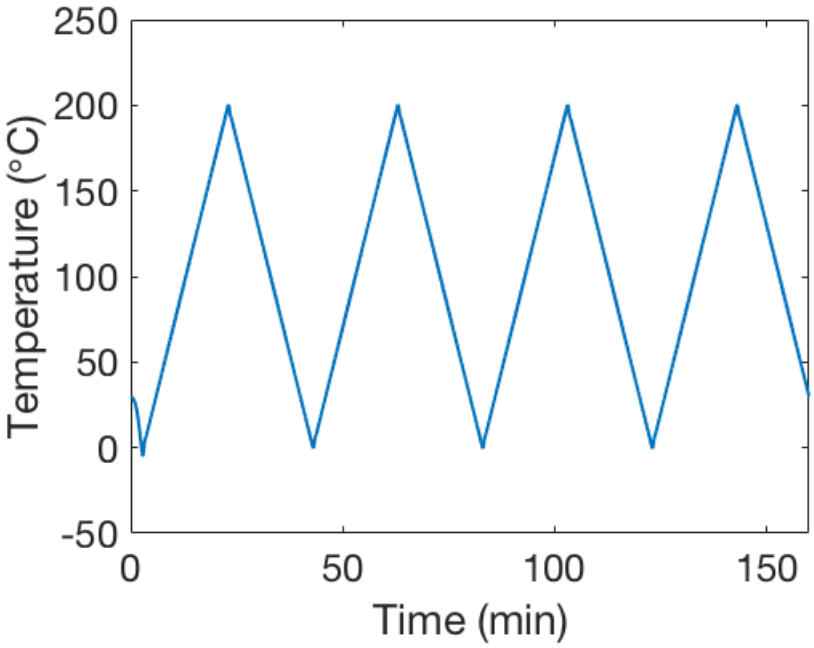

Figure 20: The temperature profile used for the DSC measurements.

3.3.4 Thermogravimetric analysis

Thermogravimetric analysis was carried out using a STA 449 F3 Jupiter to obtain values of the thermal stability of the samples. A background of an empty crucible was first collected. The samples were weighted, placed into the crucible, and then introduced into the furnace. The samples were then heated from 25 to 150 °C where it went through a isothermal step for 30 minutes. The purpose of the isothermal step is to get more exact data of the mass loss of the samples, as it helps stabilize the

weight, and therefore gives a better starting point. The samples was heated to 900 °C after the isothermal step, at a heating rate of 2 °C/min. The temperature profile is illustrated in Figure 21.

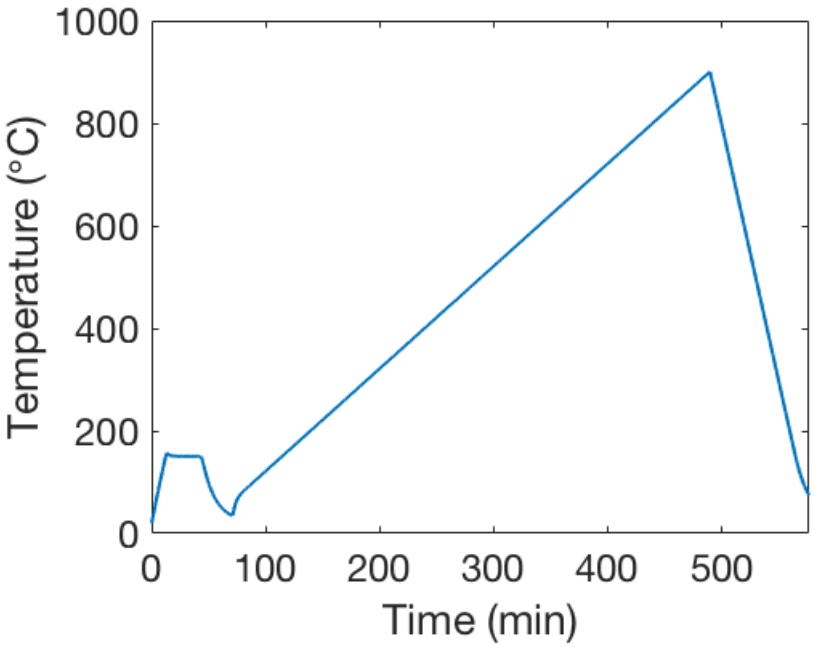

Figure 21: The temperature profile used for the TGA measurements.

3.3.5 Dielectric spectroscopy

Before performing the measurements each samples was prepared and sputtered with gold particles. A grinding machine (Labopol) was used to smooth both the top and bottom surface of the nanocomposite samples. SiC paper with graining 800, 1200 and 2400) was used for the grinding. After the grinding each sample was sputtered with a gold electrode. A multimeter was then used to make sure that the resistance of the sputtered surfaces was 5 Ω or less. The diameter and the height of the samples was measured, and while the diameter was the same for all the samples (30 mm), the height varied from sample to sample between 4.73 to 5.33 mm.

The impedance spectroscopy was carries out using a Novocontrol instrument.

The measurements was carried out using a alpha beta analyser, were the samples was placed in a Novotherm oven. A frequency range of 0.1 Hz to 1 Mhz, and an applied field of 0.1 V/mm was used to obtain the dielectric porperties of the samples. All measurements was carried out at room temperature.

4 Results

4.1 Synthesis

Can see from Figure 22 there there are large amounts of air bubbles trapped inside the composite. Figure 22A and 22B shows one side of the sample, and Figure 22C and 22D shows the other side.

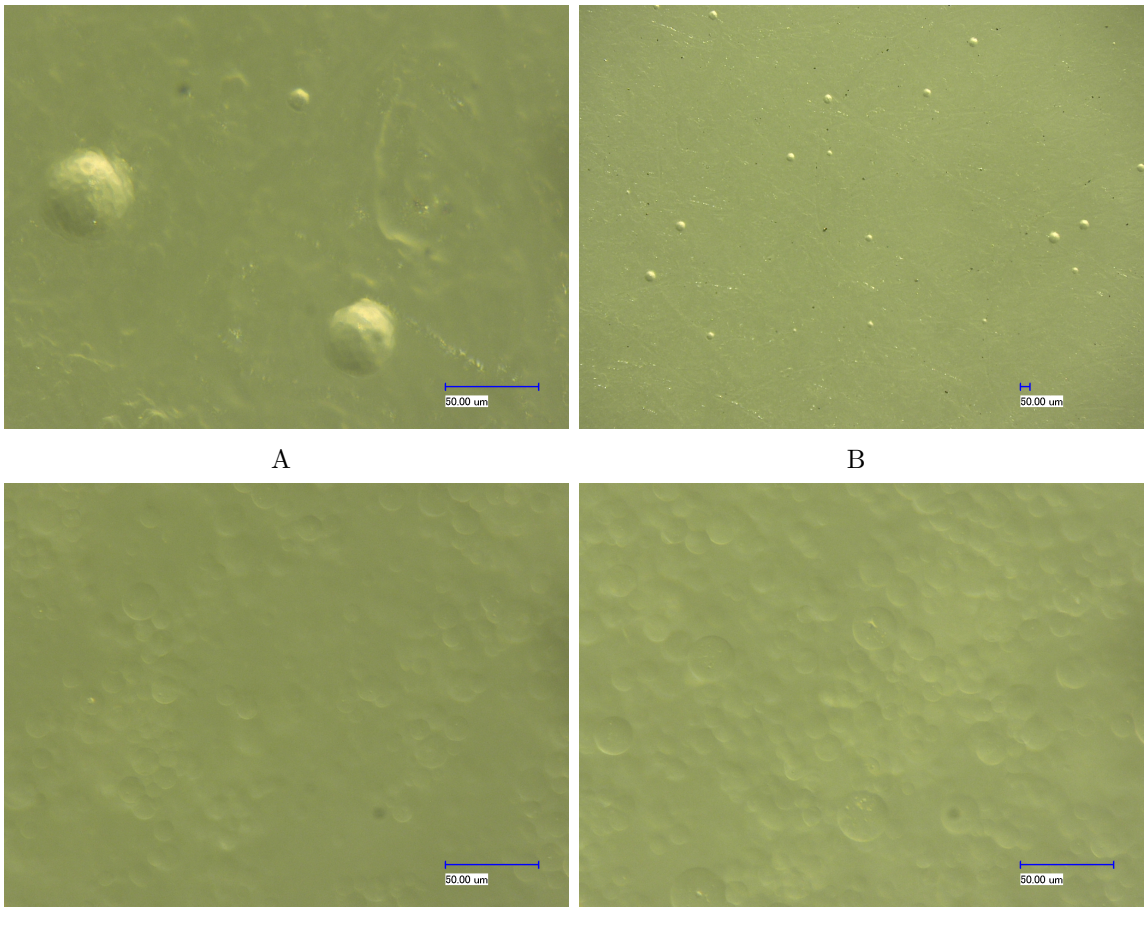

A B

C D

Figure 22: Illustration of the surface of sample with 3 wt% filler content.

4.2 Characterization of nanocomposites

4.2.1 Fourier-transform infrared spectroscopy

The FTIR spectra of the 1, 3 and 5 wt% samples, and neat epoxy, is shown in Figure 23, and the observed absorption bands are listed in Table 8. The wavelength of the different assignments is illustrated more detailed in Figure 24. The broad band ranging from 3100-3550 cm^{-1} in Figure 24A, with a peak at approximately 3350 cm^{-1} confirms the stretching vibrations of hydroxyl (OH-) groups attached to titanium [46, 47]. The large peak at 917 cm^{-1} in Figure 24B for the neat epoxy confirms the C-O bonds of the oxirane ring in the polymer [48]. For the three nanocomposite samples in Figure 24B, a broad peak can be observed in the 915-955 cm^{-1} region the appearance of vibrations due to Ti-O-Si bonds occurs [48, 46, 47]. Three distinct peaks at 2866, 2922 and 2965 cm^{-1}, shown in Figure 24C ar vibrations caused by the alkyl groups of the epoxy [46]. At approximately 1370 cm^{-1} it can be observed in Figure 24D small peaks for the three samples, which does not occur for the neat epoxy. This peak indicates the C-N bonds, which confirms the connection of the silane couling agent an the epoxy resin [46]. The peak at 805 cm^{-1} confirms that there has been formed of Ti-O-Ti [48, 47], and thus the presence of TiO_2 in the nanocomposite.

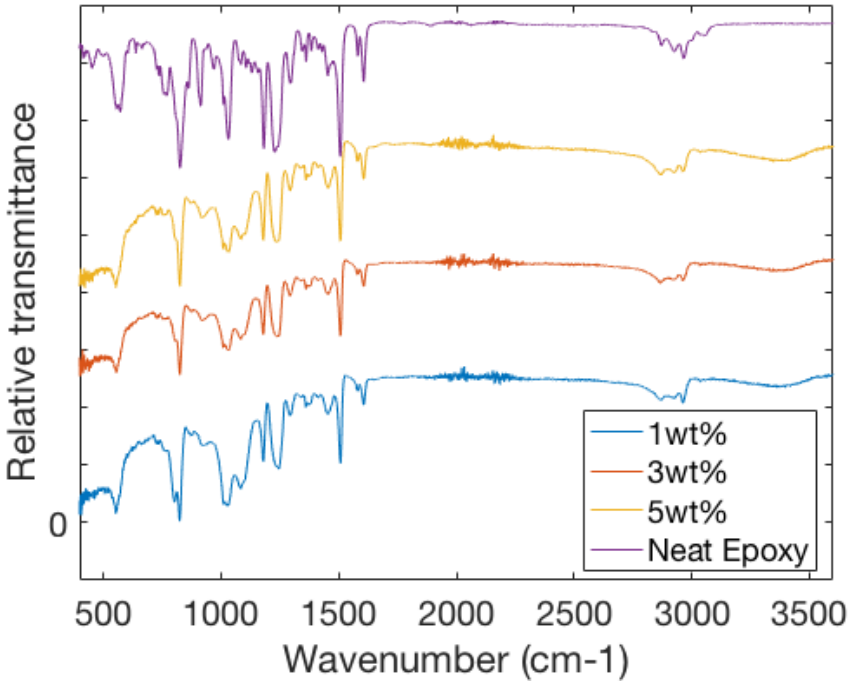

Figure 23: FTIR spectra of neat epoxy, and epoxy-TiO_2 composites with a filler content of 1, 3 and 5 wt%.

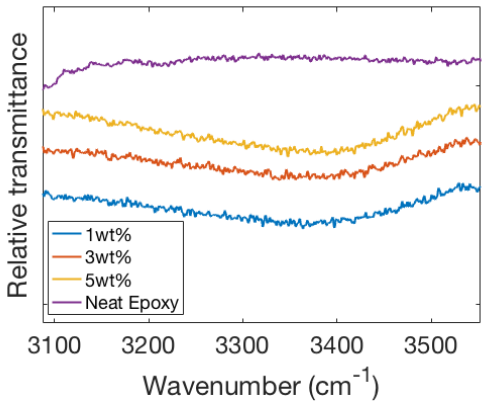

A

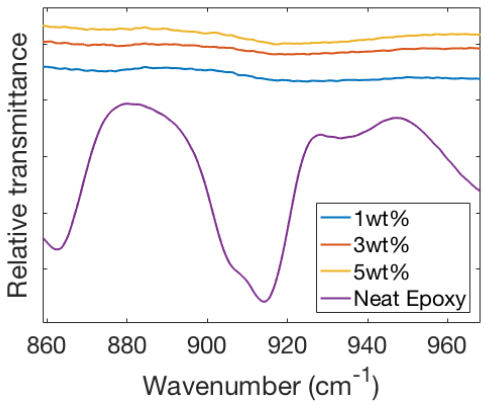

B

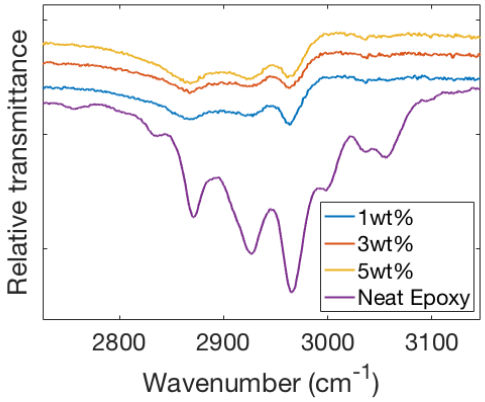

C

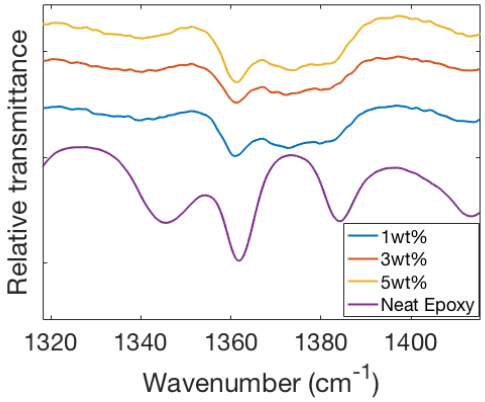

D

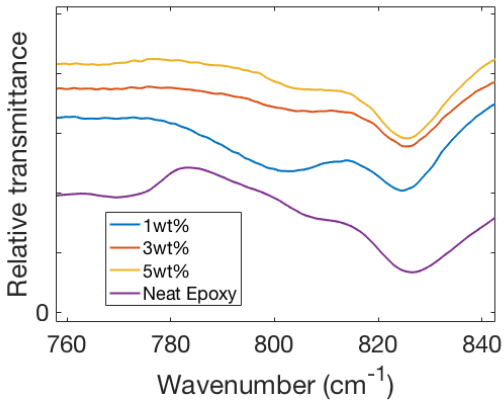

E

Figure 24: A closer look at the areas in Figure 23 of interest.

Assignment	Wavelength (cm^{-1})	Referance
O-H	3150-3550	[46, 47]
Ti-O-S	915-950	[48, 46, 47]
-CH_2	2866, 2922, 2964	[46]
Epoxide ring	917	[48]
C-N	1378	[46]
Ti-O-Ti	807	[48, 47]

Table 8: Assignment of IR bands characteristic for epoxy-TiO_2 composites.

4.2.2 Raman spectroscopy

Raman spectra of nanocomposites of 1, 3, and 5 wt%, and neat epoxy is shown in Figure 25. The marked area is magnified and displayed in Figure 26.

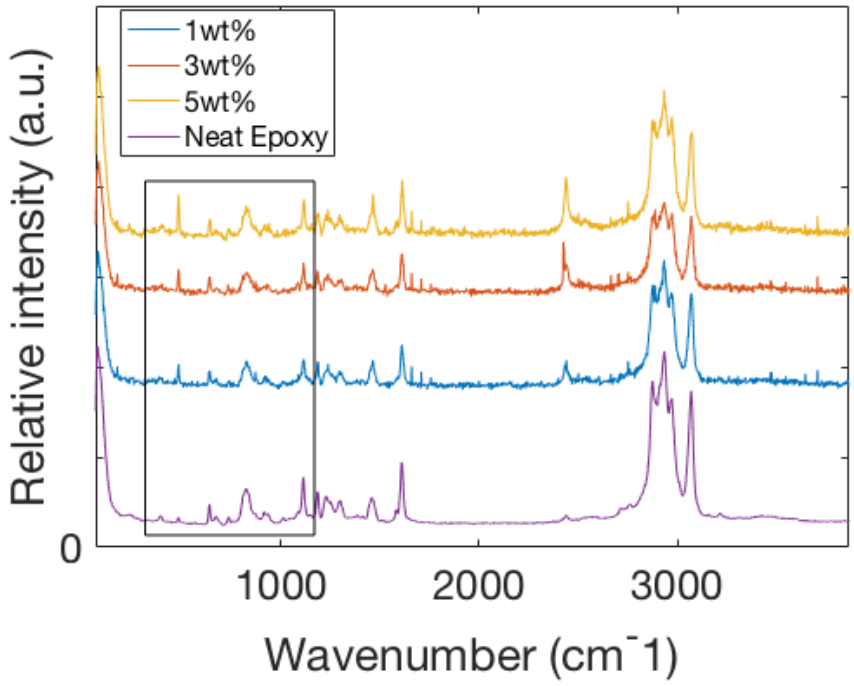

Figure 25: Raman spectra of neat epoxy, and epoxy-TiO_2 composites with a filler content of 1, 3 and 5 wt%.

From Figure 26 the expected points where the vibrations of anatase should occur is shown, at 399, 515 and 639 cm^{-1}, respectively [47]. The wavelengths at which Ti-O-Si symmetric and antisymmetric vibrations should occur are at 835 and 1030 cm^{-1} [47]. For both of these vibration types, the neat epoxy also exhibit these peaks.

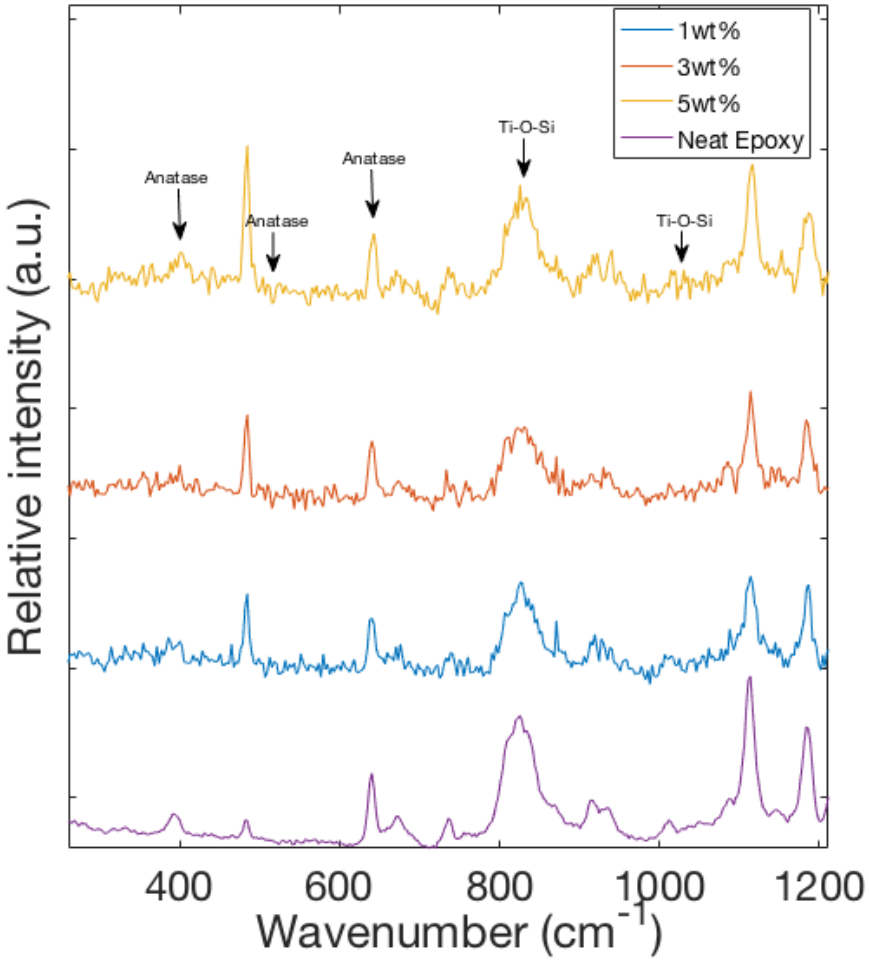

Figure 26: Enlarged spectra from 350-1200 cm^{-1}, obtained from Figure 25.

4.2.3 Differential scanning calorimetry

The glass transition temperature of the different nanocomposites, and the neat epoxy, was obtained by measuring the point of inflection of each curve, as illustrated in Figure 17. The result were obtained from Figure 27, and is listed in Table 3. There is no observed no trend amongst the different samples, other than that the 1, 3, 4 and 5 wt% samples has a higher, glass transition temperature compared to the neat epoxy. The 2 wt% sample has a lower, but not very significant, glass transition temperature.

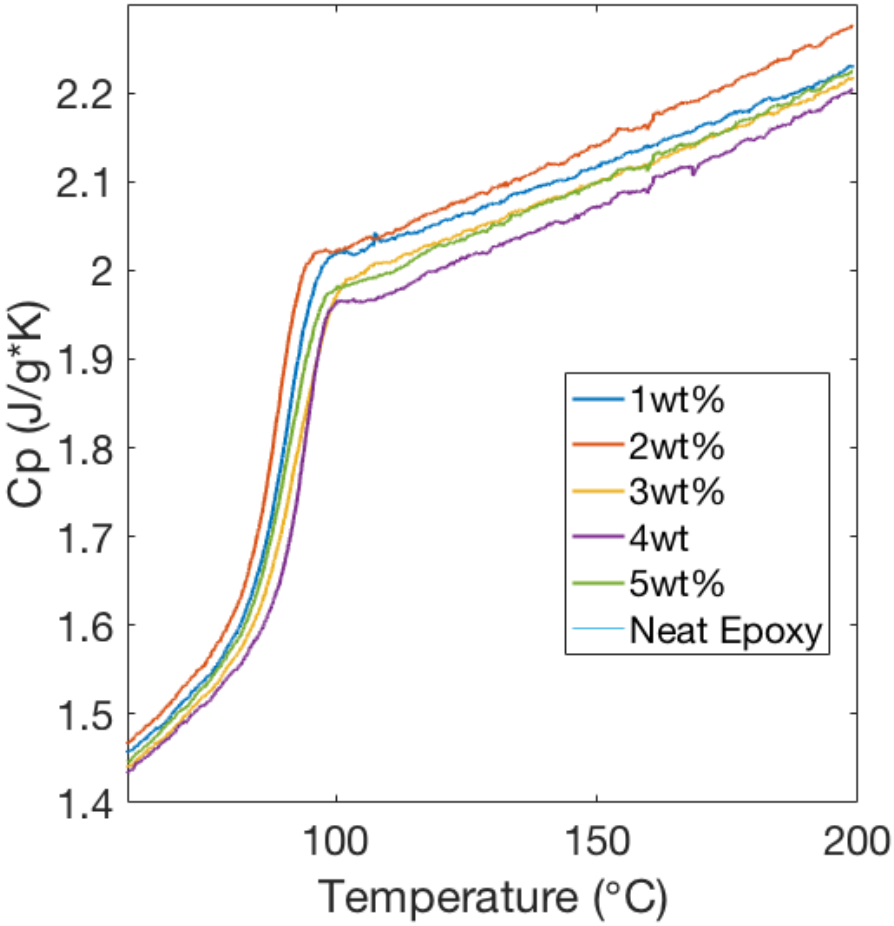

Figure 27: Changes in heat capacity as a function of temperature for neat epoxy, and nanocomposited with varying degree of filler material.

Table 9: Obtained glass transition temperature values from Figure 27.

Sample	T_g(°C)
1 wt%	90.18
2 wt%	88.09
3 wt%	93.12
4 wt%	93.42
5 wt%	90.56
Epoxy	89.55

4.2.4 Thermogravimetric analysis

The degredation of the different samples prepared is illustrated in Figure 28. The degradation of all the prepared samples, 1-5 wt%, is initiated at 317 °C. As for the neat epoxy, the initiation starts at 325 °C.

All the prepared samples, as well as the neat epoxy, shows the same mass loss pattern, with two distinct degradation stages, (I) and (II). Most of the mass is lost in the first degradation stage, which occurs at 320-440 °C. At the second degradation stage the degradation of the prepared nanocomposites occurs at 440-490 °C, while it for the neat epoxy occurs at 410-535 °C. Table 10 gives the remaining mass from each sample. A closer look at the remaining mass of the different samples is shown in Figure 29. The 4 wt% samples shows the highest remaining mass at approximately 6.19 %, while the neat epoxy shows the lowest remaining mass with roughly 0.35 %.

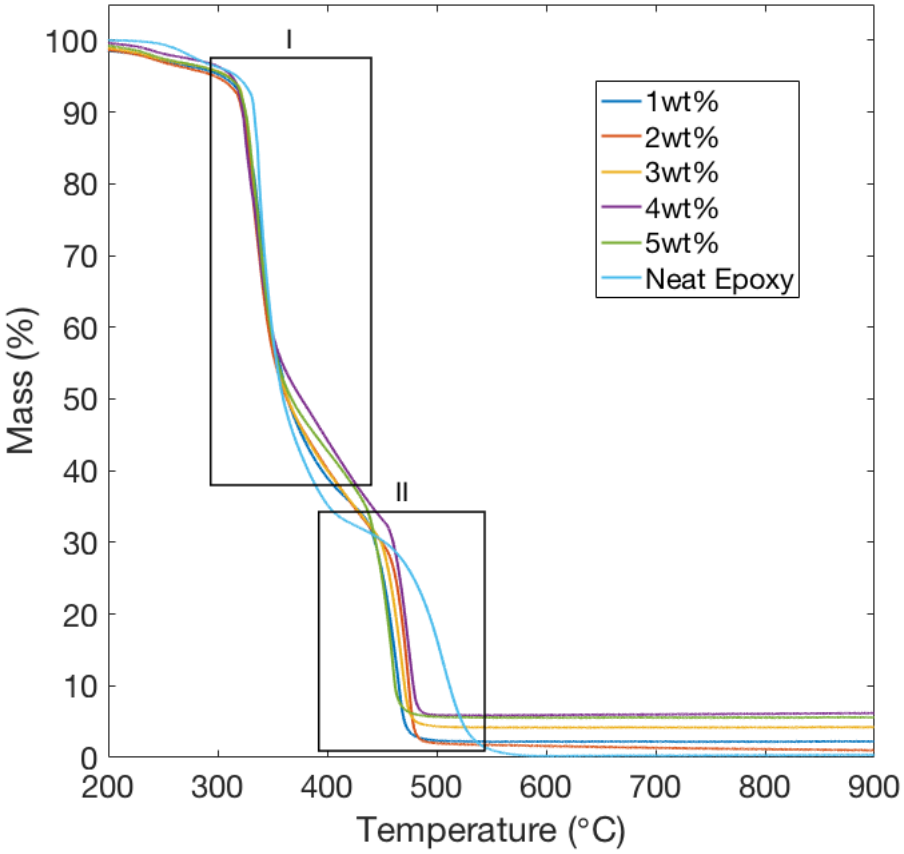

Figure 28: Mass loss of neat epoxy, and epoxy-TiO_2 composites with a filler content of 1, 2, 3, 4 and 5 wt%, as a function of temperature. The two degradation stages as outlined.

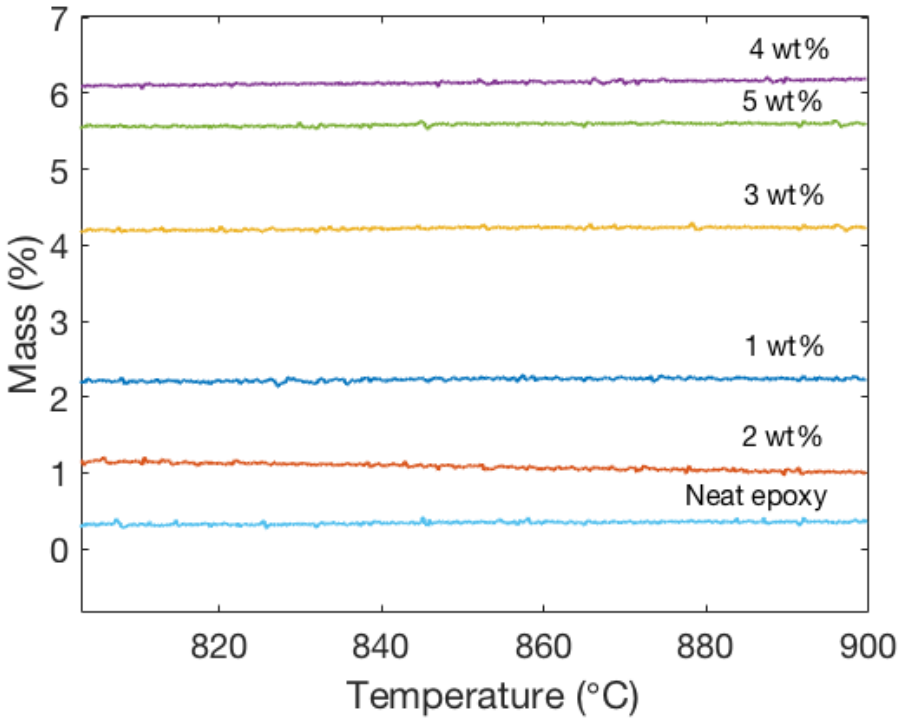

Figure 29: The remaining mass after the thermogravimetric analysis is completed.

Sample code	**Mass (%)**
1 wt%	2.23
2 wt%	1.0
3 wt%	4.23
4 wt%	6.19
5 wt%	5.56
Neat epoxy	0.35

Table 10: Remaining mass after the thermogravimetric analysis for neat epoxy, and epoxy-TiO_2 composites with a filler content of 1, 2, 3, 4 and 5 wt%.

4.2.5 Impedance spectroscopy

4.2.5.1 Relative permittivity

Figure 30 illustrates the relative permittivity of the composites, as well as neat epoxy, in the frequency range of 0.1 Hz to 1 MHz. All the samples shows the same trend of decreasing relative permittivity with increasing frequency. At around 1 Hz the relative permittivity lies in the range of 5.15 to 5.4 for the different samples, and they experience an decrease in relative permittivity with roughly 0.5.

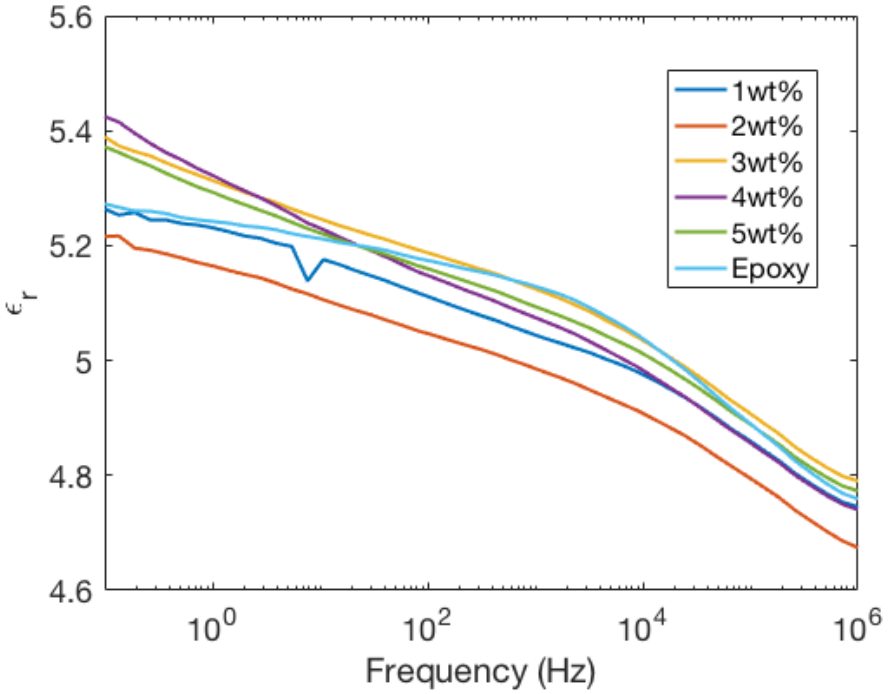

Figure 30: Relative permittivity of neat epoxy, and epoxy-TiO_2 composites with a filler content of 1, 2, 3, 4 and 5 wt%.

4.2.5.2 Dielectric loss

The dielectric losses are displayed in Figure 31. All the samples experiences an increase in the value of tanδ

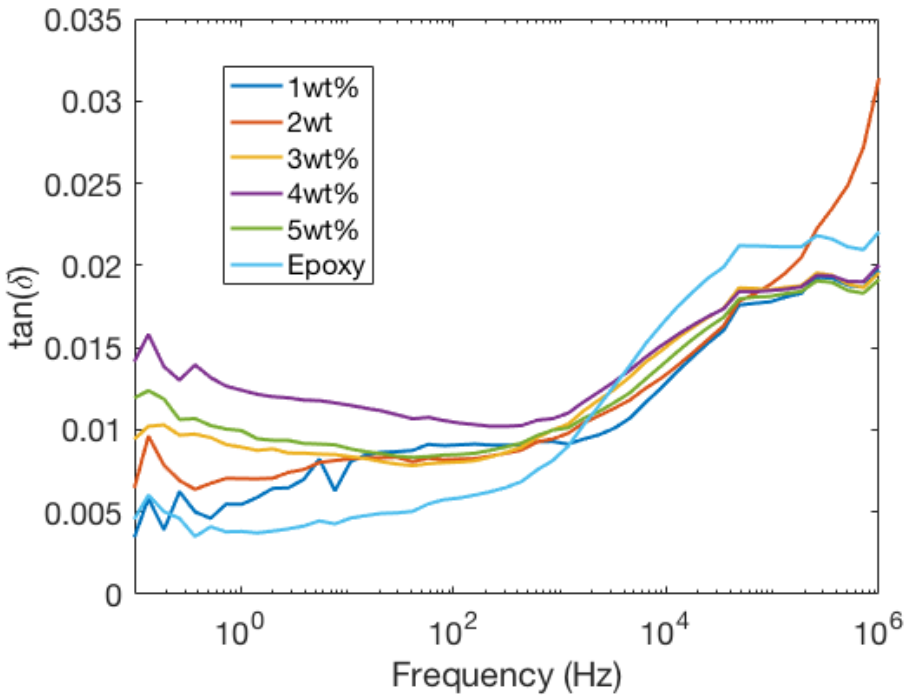

Figure 31: .

4.2.6 Small angle X-ray scattering

The scattering profiles of the SAXS measurements are displayed in Figure 32. The different samples displays the same patterns, and can therefore be assumed isotropic [47]. There is no peaks that can be observed in this plot that confirmes the precence of TiO_2, as the dataset does not include those values. However, at the end of the plot, all the samples seems to start to curve, which would be expected for epoxy composites containing TiO_2 [49].

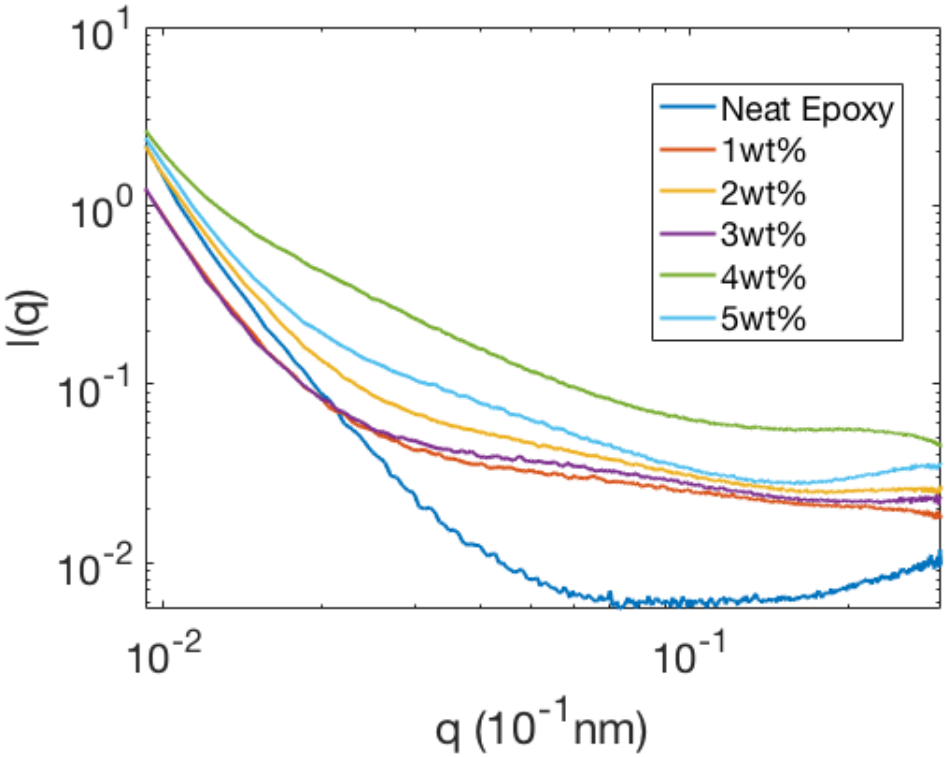

Figure 32: SAXS scattering profiles (Guinier plot) of neat epoxy, and epoxy-TiO_2 composites with a filler content of 1, 3 and 5 wt%.

5 Discussion

5.1 Fourier-transform infrared sprectroscopy

The FTIR spectra confirms the presence of Ti-O-Ti bonds, which indicates that there is synthesized TiO_2 particles directly inside the epoxy matrix. The *in situ* sol-gel synthesis route provides therefore a method to prepare hybrid composites. As there is no signal for the oxirane ring for the samples, it indicates that the ring is broken and that the monomer might have bonded with the silane coupling agent. This is also a necessity as the monomer is not able to polymerize by themselves to form the polymer matrix. The bonding is confirmed as there is detected a signal typical for C-N around 1370 cm^{-1}. The presence of Ti-O-Si bonds confirms that the silane coupling agent also have gone through a condensation reaction and coupled with the TiO_2. The silane coupling agent is therefore confirmed to have connected the inorganic TiO_2 particles with the polymer network.

5.2 Raman

The expected peaks that confirms the presence of TiO_2 are visible in Figure 26, but they do also show for neat epoxy. This might be caused by the amounts of filler material, and how they are to small to be detected compared to the vibrations of the neat epoxy.

5.3 Glass transition temperature

The glass transition temperature when incorporating a filler material, as listed in Table 9 show an increase compared the neat epoxy, but for one sample. The composite with 2 wt% filler content experience a lower, but not significantly lower glass transition temperature. As for the composite samples there are no trends in the temperature as one would expect in terms of the literature, where increasing filler

content gives higher glass transition temperature, as it limits the movement of the polymer chains. The measured glass transition temperature for neat epoxy correlates well with the literature, but as listed in Table **??**, the values varies with as much as 20 °C. There are several factors that might affect the glass transition temperature of the composites, such as synthesis method, choice of silane coupling agent, but most likely the quality of the dispersion affects the temperature the most. If the quality of the dispersion is low, e.g. not very homogeneous, the networking in the polymer may be reduced, and as a consequence the mobility of the material. Increased mobility leads to decreasing glass transition temperature.

5.4 Degradation

As seen in Figure 28, the degradation curve is almost identical for all the prepared samples compared to neat epoxy. There is no significant differences, but the samples show no increase in thermal stability, as the degradation is initiated at a earlier stage, compared to the neat epoxy. While one would expect higher thermal stability for epoxy-SiO_2 composite cause by the high thermal stability of silica, this is not the case for the epoxy-TiO_2 composite. This is most likely due to oxidative decomposition pathways attributed to the composite, which is caused by metal-catalyzation. The degradation of a material depends on many different variables, but most notable is the amount degree of dispersion, amount of impurities, and/or also the oxygen contamination. Most of the degradation happens in the first degradation stage, which most likely is polymers being burnt off. The second degradation stage follows shortly after the first stage, and in the temperature range 350-490 °C, more than 90 % of the mass, of every sample, has been pyrolyzed. This is as expected, as most types of polymers are decomposed before the temperature reach 700 °. The remaining mass should therefore be of inorganic nature, and in this case TiO_2, as the temperature need to exceed 1000 °C for inorganic materials to be pyrolyzed completely. The remaining masses do not make much sense, as it should be expected that the 5 wt% sample should have the highest remaining mass, and the 1 wt% the lowest. The reason for this might be poor quality of dispersion, or that not all of the precursor have reacted

to form the TiO_2 nanoparticles.

5.5 Relative permittivity

As seen in Figure 30, there is no significant difference in the relative permittivity of the samples compared to neat epoxy. For epoxy-TiO_2 composites with samples containing 1-5 wt% TiO_2 nanoparticles there is expected an decrease in the relative permittivity [18]. This is the case for 1, 2 and 4 wt% of filler content, but not for 3 and 5 wt%. The reason for this might be agglomerations of the TiO_2, or the size of the TiO_2 particles, as the might be of microsize. Epoxy-TiO_2 composites with particles of microsize have shown to increase the relative permittivity compared to neat epoxy. Since the samples lies both over and under the neat epoxy, there might be a big size sitribution of the TiO_2 particles, as they show no significant difference in relative permittivity compared to the neat epoxy.

5.6 Dielectric losses

From Figure 31 the samples containing 1, 3, 4 and 5 wt% of filler materials shows an increase in the loss tangent compared to the neat epoxy, in the range 0.1-1000 Hz, but a decrease of the loss tangent in the range 1000 Hz to 1 MHz. This is a desired feature as the dielectric loss is desired to be as low ass possible, as dielectric heating is unwanted. The sample containing 2 wt% of filler material shows the same trend as the other samples, but increases compared to the neat epoxy at around 0.26 MHz.

5.7 Small-angle X-ray scattering

The large slope indicates large scattering, and therefore confirms some agglomerations or domains in the composite material. However, it is not possible to confirm whether it is TiO_2 nanoparticles or not, as the data is not sufficient. There should be expected peaks at 2 nm^{-1} [49] for the TiO_2 particles.

6 Conclusion

In this master thesis an *in situ* sol-gel synthesis route were applied to produce hybrid nanocomposites of inorganic and organic material. The material was prepared using bisphenol A diglycidyl (DGEBA) ether as a organic matrix, titanium(IV)isopropoxide (TIP) as the inorganic precursor, and (3-Aminopropyl)triethoxysilane as a coupling agent to connect the two materials. The prepared samples were then characterized to investigate if there were any changes in properties related to electrical applications.

As the FTIR confirmed the presence of TiO_2 in the material, it can be concluded that the *in situ* sol-gel route is promising viable way to obtain hybrid materials. The different characterization techniques applied indicates that there are still more work to be done, as they give no clear indication on how the nanoparticles affect the properties of the polymer material.

7 Future work

In terms of developing a synthesis method for a hybrid composite material *in situ* with the use of the sol-gel method, the results are promising. The characterization result however, gives an indication that there are room for improvement in terms of the synthesis. As the quality of the dispersion is very important in terms of the properties of the hybrid composite, continuously work on perfecting the synthesis parameters should be carried out. As the SAXS did not have the data for the desired sizes of the nanoparticles, it did not confirm if there was in fact any TiO_2 in the polymer. It should therefore be done more SAXS measurements for bigger data sets.

Bibliography

[1] T. Tanaka, G. C. Montanari, and R. Mulhaupt. *IEEE Trans. Diel. and Elec. Insul.*, 11(5):763–784, 2004.

[2] M. Adnan, A. Dalod, M. Balci, J. Glaum, and M-A. Einarsrud. In situ synthesis of hybrid inorganic-polymer nanocomposites. *Polymers*, 10:1129, 2018.

[3] E. A. J. Bleeker et al. Considerations on the EU definition of a nanomaterial: Science to support policy making. *Regulatory Toxicology and Pharmacology*, 65:119–125, 2013.

[4] E. Roduner. Size matters: why nanomaterials are different. *Chem. Soc. Rev.*, 35(7):583–592, 2006.

[5] K. Y. Lau and M. A. M. Piah. Polymer nanocomposites in high voltage electrical insulation perspective: A review. *Malaysian Polymer Journal*, 6(1):58–69, 2011.

[6] Z. Cai, Q. Yao, X. Chen, and X. Wang. *Nanomaterials With Different Dimensions for Electrocatalysis*. Elsevier, Radarweg 29, 1043 NX Amsterdam, The Netherlands, 2019.

[7] Ibrahim Khan, K. Saeed, and Idrees Khan. Nanoparticles: Properties, applications and toxicities. *Arabian Journal of Chemistry*, 2017.

[8] H. Zhang and J. F. Banfield. Structural characteristics and mechanical and thermodynamic properties of nanocrystalline TiO_2. *Chem. Rev.*, 114(19):9613–9644, 2014.

[9] A. Fujishima and K. Honda. Electrochemical photolysis of water at a semiconductor electrode. *Nature*, 238:37–38, 1972.

[10] X. Chen and S. S. Mao. Titanium dioxide nanomaterials: Synthesis, properties, modifications, and applications. *Chem. Rev.*, 107:2891–2959, 2007.

[11] D. Reyes-Coronado, G. R. Gattorno, M. E. Pesqueira, C. Cab, R. de Coss, and G. Oskam. Phase-pure TiO_2 nanoparticles: Anatase, brookite and rutile. *Nanotechnology*, 19(14):145605, 2008.

[12] M. Landmann, E. Rauls, and W. G. Schmidt. The electronic structure and optical response of rutile, anatase and brookite TiO_2. *J. Phys.: Condens. Matter*, 24:195503, 2012.

[13] D. Dambournet, I. Belharouak, and K. Amine. Tailored preparation methods of TiO_2 anatase, rutile, brookite: Mechanism of formation and electrochemical properties. *Chem. Mater.*, 22(3):1173–1179, 2010.

[14] S. Fakirov. *Part 1: Introduction*. John Wiley Sons, Hoboken, New Jersey, USA, 2017.

[15] J. H. Koo. *Selecting Epoxy Resin and Nanoparticles for Applications*. McGraw-Hill, New York, New York, USA, 2006.

[16] W. W. Graessley. Entangled linear, branched and network polymer systems - Molecular theories. *Polymer*, 47:67–117, 1982.

[17] L. Shan, K. N. E. Verghese, C. G. Robertson, and K. L. Reifsnider. Effect of network structure of epoxy dgeba-poly(oxypropylene)diamineson tensile behavior. *Journal of Polymer Science*, 37:2815–2819, 1999.

[18] M. Adnan, E. G. Tveten, J. Glaum, M-H. G. Ese, S. Hvidsten, Wilhelm W. Glomm, and M-A. Einarsrud. Epoxy-based nanocomposites for high-voltage insulation: A review. *Adv. Elec. Mater.*, 5:1800505.

[19] R. Kochetov, T. Andritsch, P. H. F. Morshuis, and J. J. Smit. Anomalous behaviour of the dielectric spectroscopy response of nanocomposites. *IEEE Trans. Diel. Elec. Insul.*, 19(1):107–117, 2012.

[20] J. Jiao, P. Liu, L. Wang, and Y. Cai. One-step synthesis of improved silica/epoxy nanocomposites with inorganic-organic hybrid network. *Journal of Polymer Science*, 20(8):202, 2013.

[21] S. Siddabattuni, T. P. Schuman, and F. Dogan. Dielectric properties of polymer–particle nanocomposites influenced by electronic nature of filler surfaces. *ACS Appl. Mater. Interfaces*, 5(6):1917–1927, 2013.

[22] I. Pleşa, P. V. Noţingher, S. Schlögl, C. Sumereder, and M. Muhr. Properties of polymer composites used in high-voltage applications. *Polymers*, 8(5):2073–4360, 2016.

[23] W. R. Ashcroft. *Curing agents for epoxy resins*. Springer Netherlands, Dordrecht, 1993.

[24] M. Adnan, A. Dalod, M. Balci, J. Glaum, and M-A. Einarsrud. In situ synthesis of hybrid inorganic-polymer nanocomposites. *Polymers*, 10:1129, 2018.

[25] F. Torrens and G. Castellano. Bisphenol, diethylstilbestrol, polycarbonate and the thermomechanical properties of epoxy–silica nanostructured composites. *J. Resea. Upda. Pol. Sci.*, 2(4):183–193, 2013.

[26] H. Zou, S. Wu, and J. Shen. Polymer/silica nanocomposites: Preparation, characterization, properties, and applications. *Chem. Rev.*, 108(9):3893–3957, 2008.

[27] Y. Wang. *Special nanomaterials*. World Scientific, Singapore, 2011.

[28] C. Sanchez, B. Julián, P. Belleville, and M. Popall. Applications of hybrid organic–inorganic nanocomposites. *Journal of Materials Chemistry*, 15(35-36):3559–3592, 2005.

[29] G. Schottner. Hybrid solgel-derived polymers: Applications of multifunctional materials. *Chem. Mat.*, 13(10):3422–3435, 2001.

[30] P. Judeinstein and C. Sanchez. Hybrid organic–inorganic materials: a land of multidisciplinarity. *J. Mater. Chem.*, 6(4):511–525, 1996.

[31] C. Sanchez, F. Ribot, and B. Lebeau. Molecular design of hybrid organic-inorganic nanocomposites synthesized via sol-gel chemistry. *J. Mater. Chem.*, 9(1):35–44, 1999.

[32] J. K. Nelson, J. C. Fothergill L.A. Dissado, and W. Peasgood. Towards an understanding of nanometric dielectrics. *Conf. Electron. Insul. Dielectr. Pheno.*, 1:295–298, 2012.

[33] S. Singha and M. J. Thomas. Dielectric properties of epoxy nanocomposites. *IEEE Trans. Diel. Elec. Ins.*, 15(1):12–23, 2008.

[34] W. S. Khan, N. N. Hamadneh, and W. A. Khan. *Polymer nanocomposites – synthesis techniques, classification and properties.* OCP, Atlantic Street, Altrincham, Cheshire, United Kingdom, 2017.

[35] W. R. Caseri. Nanocomposites of polymers and inorganic particles: preparation, structure and properties. *Mat. Sci. Tech.*, 22(7):807–817, 2006.

[36] H. Althues, J. Henle, and S. Kaskel. Functional inorganic nanofillers for transparent polymers. *Chem. Soc. Rev.*, 36(9):1454–1465, 2007.

[37] C. Ü and Y. Bai. High refractive index organic–inorganic nanocomposites: design, synthesis and application. *J. Mater. Chem.*, 19(19):2884–2901, 2009.

[38] A. E. Danks, S.R. Hall, and Z. Schnepp. The evolution of 'sol–gel' chemistry as a technique for materials synthesis. *Mater. Horiz.*, 3(2):91–112, 2016.

[39] F. Bellucci, D. Fabiani, G. C. Montanari, and L. Testa. *The Processing of Nanocomposites.* Springer US, Boston, MA, 2010.

[40] Chemat Group. Sol-gel technology and products, 2018.

[41] S. Kango, S. Kalia, A. Celli, J. Njuguna, Y. Habibi, and R. Kumar. Surface modification of inorganic nanoparticles for development of organic–inorganic nanocomposites—a review. *Progress in Polymer Science*, 38(8):1232–1261, 2013.

[42] S. Kango, S. Kalia, A. Celli, J. Njuguna, Y. Habibi, and R. Kumar. Surface modification of inorganic nanoparticles for development of organic–inorganic nanocomposites - a review. *Progress in Polymer Science*, 38(8):1232–1261, 2013.

[43] S. Shokoohi, A. Arefazar, and R. Khosrokhavar. Silane coupling agents in polymer-based reinforced composites: A review. *J. Reinf. Plast. and Comp.*, 27(5):473–485, 2008.

[44] M.S. Goyat, S. Rana, Sudipta Halder, and P.K. Ghosh. Facile fabrication of epoxy-tio2 nanocomposites: A critical analysis of tio2 impact on mechanical properties and toughening mechanisms. *Ultrasonics Sonochemistry*, 40:861–873, 2018.

[45] R. J. D. Tilley. *Insulating solids.* John Wiley Sons, Ltd, Hoboken, New Jersey, USA, 2004.

[46] D. Meroni et al. A close look at the structure of the TiO_2-aptes interface in hybrid nanomaterials and its degradation pathway: An experimental and theoretical study. *J. Phys. Chem. C*, 121(1):430–440, 2017.

[47] A. R. M. Dalod. *In situ synthesis of titania and titanium based organicinorganic nanomaterials.* PhD thesis, Norwegian University of Science and Technology, Trondheim, Norway, 2017.

[48] A. R. M. Dalod, L. Henriksen, T. Grande, and M-A. Einarsrud. Functionalized TiO_2 nanoparticles by single-step hydrothermal synthesis: the role of the silane coupling agents. *Beilstein J. Nanotechnol.*, 8:304–312, 2017.

[49] Y. Shoichiro et al. Properties and microstructures of epoxy resin/TiO_2 and SiO_2 hybrids. *Polymer International*, 54:354–361, 2005.

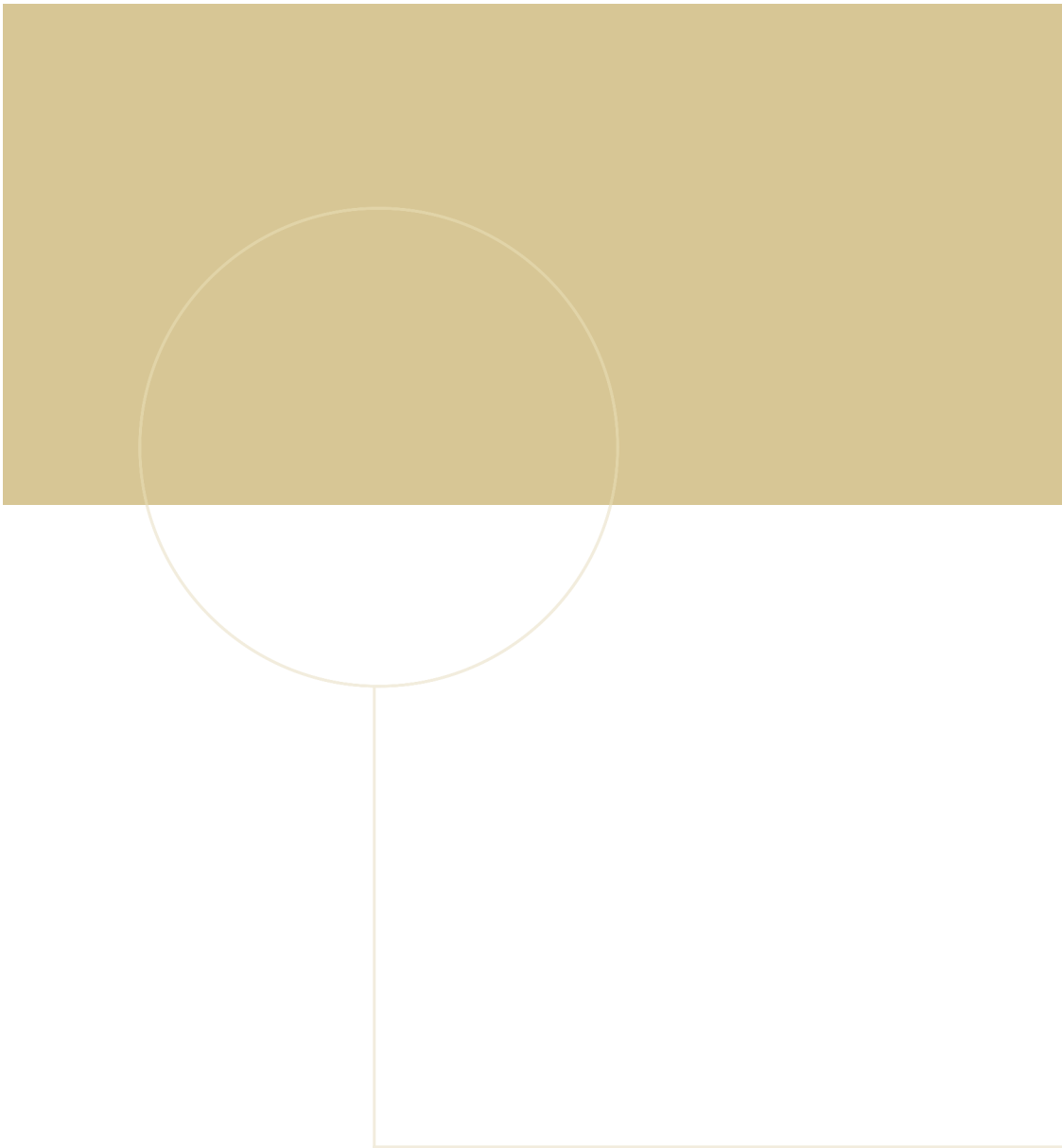

NTNU
Norwegian University of
Science and Technology